

VoLTA: VISION-LANGUAGE TRANSFORMER WITH WEAKLY-SUPERVISED LOCAL-FEATURE ALIGNMENT

Shraman Pramanick^{*1}, Li Jing^{*2}, Sayan Nag^{*3}, Jiachen Zhu⁴, Hardik Shah²,
Yann LeCun^{2,4}, Rama Chellappa¹

¹Johns Hopkins University ²Meta AI ³University of Toronto ⁴New York University
 {spraman3, rchella4}@jhu.edu, {ljng, hjshah}@fb.com
 sayan.nag@mail.utoronto.ca, {jiachen.zhu, yann.lecun}@nyu.edu



Figure 1: We introduce VoLTA, Vision-Language Transformer with weakly-supervised local-feature Alignment, a VLP paradigm trained with graph optimal transport (GOT) based *image-text* matching. VoLTA learns fine-grained local visual representation only using global *image-caption* pairs, eliminating the use of expensive grounding annotations. **This figure shows how different words in captions attend relevant image regions, produced by the GOT module of VoLTA pre-trained on COCO.**

ABSTRACT

Vision-language pre-training (VLP) has recently proven highly effective for various uni- and multi-modal downstream applications. However, most existing end-to-end VLP methods use high-resolution image-text-box data to perform well on fine-grained region-level tasks, such as object detection, segmentation, and referring expression comprehension. Unfortunately, such high-resolution images with accurate bounding box annotations are expensive to collect and use for supervision at scale. In this work, we propose VoLTA (Vision-Language Transformer with weakly-supervised local-feature Alignment), a new VLP paradigm that only utilizes image-caption data but achieves fine-grained region-level image understanding, eliminating the use of expensive box annotations. VoLTA adopts graph optimal transport-based weakly-supervised alignment on local image patches and text tokens to germinate an *explicit, self-normalized, and interpretable* low-level matching criterion. In addition, VoLTA pushes multi-modal fusion deep into the uni-modal backbones during pre-training and removes fusion-specific transformer layers, further reducing memory requirements. Extensive experiments on a wide range of vision- and vision-language downstream tasks demonstrate the effectiveness of VoLTA on fine-grained applications without compromising the coarse-grained downstream performance, often outperforming methods using significantly more caption and box annotations.

1 INTRODUCTION

Inspired by the escalating unification of transformer-based modeling in vision (Dosovitskiy et al., 2021; Liu et al., 2021; Chen et al., 2021a) and language (Devlin et al., 2019; Liu et al., 2019) domains, coupled with readily available large-scale *image-caption* pair data, vision-language pre-training

^{*}Equal technical contribution.

(VLP) (Lu et al., 2019; Li et al., 2020a; Kim et al., 2021; Kamath et al., 2021; Zhang et al., 2021) has recently been receiving ever-growing attention. VLP has not only been proven the *de-facto* for several VL tasks, but it has also been beneficial for traditional vision-only tasks, such as image classification and object detection. Such wide-range applications of VLP can broadly be categorized into two groups: (i) tasks requiring image-level understanding, e.g., image classification, image & text retrieval (Plummer et al., 2015), visual question answering (Antol et al., 2015), and (ii) tasks requiring region-level understanding, e.g., object detection, instance segmentation, and referring expression comprehension (Kazemzadeh et al., 2014; Yu et al., 2016). Most existing VLP methods support either application, leaving the question of a generalizable and unified VL framework.

Traditional VLP methods with image-level understanding (Li et al., 2021a; Wang et al., 2021b; Dou et al., 2022b) utilize large-scale *image-caption* pair datasets and are commonly trained with image-text contrastive objectives computed on global features. Hence, it is not trivial to extend such methods to region-level applications. On the other hand, VLP methods with region-level understanding (Kamath et al., 2021; Li et al., 2022b; Zhang et al., 2022) use *image-text-box* grounding data and are designed to predict bounding boxes during pre-training. Consequently, they do not support image-level tasks. Furthermore, accurate bounding box annotations require high-resolution input images, which are often expensive to collect, annotate and use for pre-training at scale. Recently, FIBER (Dou et al., 2022a) addressed the problem of such unified VLP and proposed a two-stage pre-training algorithm requiring fewer box annotations than previous region-level pre-training methods. Moving a step forward, we aim to eliminate the use of costly box annotations and ask the challenging but natural question: *Can we attain region-level understanding from global image-caption annotations and unify image- and region-level tasks in a single VL framework?*

Subsequently, we focus on achieving region-level fine-grained understanding by weakly-supervised alignment of image patches and text tokens. Previous VLP methods (Chen et al., 2020d; Kim et al., 2021) in this direction use Wasserstein distance (WD) (Peyré et al., 2019), a.k.a Earth Mover’s distance (EMD)-based optimal transport (OT) algorithms for such alignment problem. However, we argue that WD is not optimum for intricate images with multiple similar entities. Thus, we propose to jointly utilize Gromov-Wasserstein distance (GWD) Peyré et al. (2016) and Wasserstein distance (WD) in a setup known as graph optimal transport Li et al. (2019). Moreover, instead of using commonly deployed contrastive objective, we propose to utilize redundancy reduction from Barlow Twins Zbontar et al. (2021), which is less data-intensive and does not require hard-negative mining. We also follow Dou et al. (2022a) to incorporate deep multi-modal fusion into the uni-modal backbones, removing the need for costly fusion-specific transformer layers. To this end, we introduce VoLTA, Vision-Language Transformer with weakly-supervised local-feature Alignment, a unified VLP paradigm only utilizes *image-caption* annotations but achieves fine-grained region-level image understanding, eliminating the use of expensive box annotations. Figure 1 visualizes the feature-level image-text alignment. VoLTA can attend text tokens to the corresponding visual patches without relying on low-level supervision.

In summary, our contributions are three-fold. (i) We propose to use graph optimal transport for weakly-supervised feature-level patch-token alignment. (ii) We introduce VoLTA, a unified VLP paradigm for image-level and region-level applications, but pre-trained only using *image-caption* pairs. VoLTA is memory, compute, and time-efficient and can easily be scaled up with readily available large-scale *image-caption* data harvested from the web. (iii) We performed a wide range of vision- and vision-language coarse- and fine-grained downstream experiments to demonstrate the effectiveness of VoLTA compared to strong baselines pre-trained with significantly more caption and box annotations.

2 RELATED WORKS

Uni-modal Self-supervised Pre-training: In recent years, the machine learning community has observed a boom of self-supervised pre-training. In the language domain, representations learned by BERT (Devlin et al., 2019), RoBERTa (Liu et al., 2019) have become the default setting for any downstream tasks. Generative models such as GPT (Radford et al., 2019; Brown et al., 2020) have also achieved impressive few-shot/zero-shot performances on novel applications. SimCSE (Gao et al., 2021) uses contrastive learning to help learn useful sentence representations.

In the vision domain, a series of contrastive/joint-embedding methods (He et al., 2020; Chen et al., 2020c; 2021b; 2020b; Grill et al., 2020; Chen & He, 2021; Caron et al., 2021; Zbontar et al., 2021; Bardes et al., 2022; Assran et al., 2022) have outperformed supervised counterparts. Recently,

generative models such as BEiT (Bao et al., 2021) and MAE (He et al., 2022) have also achieved impressive performances with much more scalable potential.

Vision-language pre-training: Vision-language pre-training (VLP) mainly relies on *image-text* pair datasets to learn joint visual-language representations. One line of work is to train separate vision and language encoders and only fuse their representation in the representation space. CLIP (Radford et al., 2021), UniCL (Yang et al., 2022a) and ALIGN (Jia et al., 2021) use image-text contrastive loss to learn aligned representations. SLIP (Mu et al., 2021) combines self-supervised visual representation learning and contrastive multi-modal learning. M3AE (Geng et al., 2022), FLAVA (Singh et al., 2022) combines masked image modeling and masked language modeling. Another line of work is to use cross attention to fuse vision and language information in the early stage (Kamath et al., 2021; Dou et al., 2022b; Lu et al., 2019; Li et al., 2020b; Kiela et al., 2019; Kim et al., 2021; Zhang et al., 2021; Li et al., 2022a; Wang et al., 2022b). These works focus on learning semantic-level aligned vision-language representations. In addition, UniTAB (Yang et al., 2022b), OFA (Wang et al., 2022a), GLIP (Li et al., 2022b), and FIBER (Dou et al., 2022a) use expensive grounding *image-text-box* annotations to learn fine-grained aligned representations. Our work uses representation space alignment and cross-attention fusion, but we do not use any box annotation to learn robust feature-level alignments.

Unsupervised Representation Alignment: Unsupervised multi-modal alignment typically relies on specific metrics. Wasserstein distance (WD) (Peyré et al., 2019), a.k.a Earth Mover’s distance (EMD)-based optimal transport (OT) algorithms have widely been adopted to various domain alignment tasks, including sequence-to-sequence learning (Chen et al., 2019), few-shot learning (Zhang et al., 2020), knowledge distillation (Balaji et al., 2019), unsupervised domain adaptation (Balaji et al., 2019), generative networks (Han et al., 2015; Genevay et al., 2018; Mroueh et al., 2018; 2019), and multi-modal learning (Yuan et al., 2020; Chen et al., 2020d; Kim et al., 2021; Li et al., 2022c; Pramanick et al., 2022). Previous VLP methods (Chen et al., 2020d; Kim et al., 2021), which use OT-based patch-word alignment, only utilize WD. However, we argue that jointly modeling Gromov-Wasserstein distance (GWD) (Peyré et al., 2016) and Wasserstein distance (WD) results in a superior multi-modal alignment for intricate images. To the best of our knowledge, this is the first work to apply WD and GWD-based optimal transport for feature-level alignment in VLP.

3 METHOD

In this section, we present our proposed framework, VoLTA, which contains three broad modules - (i) intra- and inter-modality redundancy reduction, (ii) weekly-supervised cross-modal alignment (CMA) of local features, and (iii) cross-modal attention fusion (CMAF). Next, we introduce the fine-tuning strategies for various uni- and multi-modal downstream tasks as supported by VoLTA. An overview of different modules of VoLTA is depicted in Figure 2.

3.1 PROPOSED SYSTEM - VOLTA

3.1.1 INTRA- AND INTER-MODALITY REDUNDANCY REDUCTION

We use Barlow Twins (BT) (Zbontar et al., 2021), a non-contrastive covariance regularization as the foundational objective of VoLTA. The recent success of contrastive vision-language pre-training (VLP) (Radford et al., 2021; Li et al., 2021b; Jia et al., 2021; Kim et al., 2021; Yang et al., 2022a; Dou et al., 2022a;b) has already shown that, compared to a single modality, *image-caption* pairs offer a significantly higher-level of abstractive and semantic concepts about the training samples. However, common contrastive VLP objectives, like InfoNCE (Oord et al., 2018), are data-hungry, as they require large batch sizes and well-mined hard negatives. On the other hand, the BT objective operates on the dimensions of the embeddings across the two views of training samples. Hence, it has proven robust to batch size and can be trained using lower memory resources. In this work, we extend the BT objective for multi-modal setup.

The original BT algorithm, which operates on joint embeddings of distorted samples, was proposed only for image modality. Specifically, for each image of a batch \mathcal{X} , two distorted views are obtained using a distribution of data augmentation \mathcal{T} with disparate probabilities. These distorted images are then fed into a shared image encoder which contains a feature extraction network (e.g., ResNet (He et al., 2016)) cascaded with trainable linear projection layers, producing a batch of parallel

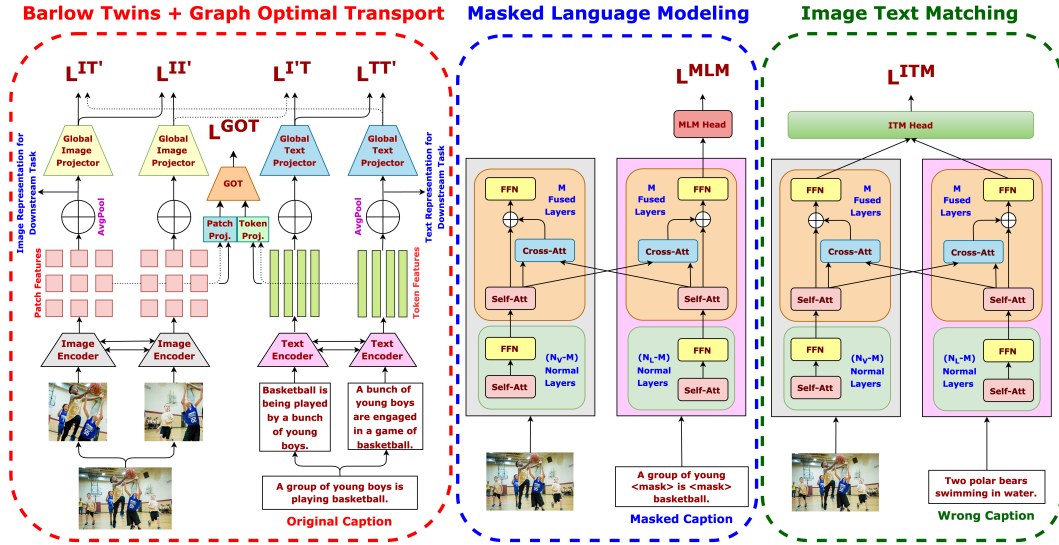


Figure 2: **Computation of four different objectives, \mathcal{L}_{BT} , \mathcal{L}_{GOT} , \mathcal{L}_{MLM} , and \mathcal{L}_{ITM} by the proposed VoLTA framework.** Inspired by (Dou et al., 2022a), VoLTA inserts cross-modal attention fusion (CMAF) inside uni-modal backbones with a gating mechanism. During VoLTA pre-training, every forward iteration consists of three steps - (i) CMAF is switched off, VoLTA acts as dual encoder, \mathcal{L}_{BT} and \mathcal{L}_{GOT} are computed. (ii) CMAF is switched on, VoLTA acts as fusion encoder, image-masked caption pair is fed into the model to compute \mathcal{L}_{MLM} . (iii) CMAF is kept on, randomly sampled image-caption pair is fed into the model to compute \mathcal{L}_{ITM} . Such fusion strategy results in a lightweight and flexible model compared to using fusion-specific transformer layers.

embeddings z^A and z^B . The BT loss computed using the encoded embeddings can be denoted as:

$$\mathcal{L}_{BT} \triangleq \sum_i (1 - C_{ii})^2 + \lambda \sum_i \sum_{j \neq i} (C_{ij})^2, \quad C_{ij} = \frac{\sum_b z_{b,i}^A z_{b,j}^B}{\sqrt{\sum_b (z_{b,i}^A)^2} \sqrt{\sum_b (z_{b,j}^B)^2}} \quad (1)$$

Where λ is a positive weighting factor; C is the cross-correlation matrix computed between z^A and z^B along the batch dimension; b stands for sample indices in a batch; i, j refers to the dimension indices of z^A and z^B . The first term in Equation 1 is the *invariance* term which attempts to equate the diagonal elements of the cross-correlation C matrix to 1, whereas the second term is the *redundancy reduction term* which pushes the off-diagonal elements of the C matrix to 0.

In this work, we propose to use BT for *image-caption* pairs. Specifically, we use stochastic data augmentations for both images and texts¹, and directly apply the BT objective for all the 2×2 pairs, resulting in additional supervision. Note that, this simple, straightforward and instinctive extension enables us to apply redundancy reduction in-between and across modalities, which intuitively results in superior visual representation. Moreover, in this bi-modal setting, we can pre-train a text encoder in parallel with the image encoder, and thus, can generalize our system to a wider range of uni- and multi-modal downstream applications.

Intra-modal Objective: Intra-modal objective refers to applying the BT loss in-between the pairs of image and text embeddings. Given an *image-caption* pair, we first have two augmented views (I, I') for each image, and two augmented views (T, T') for each text. Then, we resort to Equation 1 individually for the image and text pairs.

$$\mathcal{L}_{BT}^k \triangleq \sum_i (1 - C_{ii}^k)^2 + \lambda \sum_i \sum_{j \neq i} (C_{ij}^k)^2, \quad \forall k \in \{II', TT'\} \quad (2)$$

Inter-modal Objective: Inter-modal objective refers to applying the BT loss across the image and text embeddings. Since the image and text encoder can output features with different shapes, we design the projector layers with same output dimension. Hence, in addition to the original BT loss

¹ Image and text augmentations details can be found in Appendix D.1

between (I, I') in Zbontar et al. (2021), we get three more loss terms - (T, T') , (I, T') , (I', T) , leading to $3 \times$ diverse and high-quality additional supervision. The inter-modal BT losses can also directly be computed following Equation 1.

$$\mathcal{L}_{\text{BT}}^k \triangleq \sum_i (1 - C_{ii}^{k'})^2 + \lambda \sum_i \sum_{j \neq i} (C_{ij}^k)^2, \forall k \in \{IT', I'T\} \quad (3)$$

The resulting bi-modal BT loss is $\mathcal{L}_{\text{BT}} = \sum_k \mathcal{L}_{\text{BT}}^k, \forall k \in \{II', TT', IT', I'T\}$.

3.1.2 ALIGNMENT OF LOCAL FEATURES

Though the inter-modal redundancy reduction provides high-quality semantic supervision, it is computed on the global image- and text features and, thus, only simulates implicit and non-interpretable multi-modal alignment. However, fine-grained region-level downstream applications like detection, segmentation, and reference expression comprehension require local visual feature descriptors with specific spatial information. To achieve this, most existing top-performing VLP methods, including UniTAB (Yang et al., 2022b), OFA (Wang et al., 2022a), GLIP (Li et al., 2022b), and FIBER (Dou et al., 2022a), use high-resolution image-text-box data for fine-grained pre-training. However, bounding box annotations are expensive to collect and use for supervision. Hence, we seek an alternate weakly-supervised solution for local feature-level alignment using global image-caption annotations.

Recently, Wasserstein distance (WD) (Peyré et al., 2019), a.k.a Earth Mover’s distance (EMD)-based optimal transport (OT) algorithms have been used for weakly-supervised patch-word alignment in VLP (Chen et al., 2020d; Kim et al., 2021). Such OT-based learning methods are optimized for distribution matching by minimizing the cost of a transport plan. We pose the patch-word alignment as a more structured graph-matching problem and use the graph optimal transport (GOT) algorithm, which utilizes Gromov-Wasserstein distance (GWD) (Peyré et al., 2016) in conjunction with WD to ensure the preservation of topological information during cross-modal alignment. More specifically, we obtain the patch- and token-level features from the last layers of corresponding visual and textual transformer encoders, and use these encoded local-feature vectors to construct modality specific dynamic graphs - $\mathcal{G}_x(\mathbb{V}_x, \mathcal{E}_x)$ for image patches and $\mathcal{G}_y(\mathbb{V}_y, \mathcal{E}_y)$ for text tokens. Each node in these graphs $i \in \{\mathbb{V}_x, \mathbb{V}_y\}$ is represented by corresponding feature vectors, and intermediate edges $e \in \{\mathcal{E}_x, \mathcal{E}_y\}$ by thresholded cosine similarity.

Importance of GOT in patch-word alignment: As mentioned previously, GOT adopts two types of OT distances - WD for node matching and GWD for edge matching. In contrast, previous vision-language pre-training algorithms (Chen et al., 2020d; Kim et al., 2021) using OT for patch-word alignment only considered WD. However, we argue that intricate images with multiple similar objects with different shapes and colors require both WD and GWD for accurate, fine-grained matching. For example, in Figure 3, there are multiple “men” present in the image. WD can only match nodes in the graph, and will treat all “men” entities as identical and will ignore neighbouring relations like “*in blue shirt*” and “*holding the scissors*”. However, by using proper edge matching with GWD, we can preserve the graph’s topological structure. We can correctly identify which “*man*” in the image the sentence is referring to. Hence, we couple WD and GWD mutually beneficially and use a joint transport plan for accurate patch-word matching.

Once \mathcal{G}_x and \mathcal{G}_y are computed, we follow Chen et al. (2020a) to compute WD and GWD.

Wasserstein Distance (WD) calculates the pairwise distances between two sets of cross-domain node embeddings. Consider two discrete distributions, $\phi \in \mathbf{P}(\mathbb{X})$ and $\psi \in \mathbf{P}(\mathbb{Y})$, where $\phi = \sum_{i=1}^n u_i \delta_{x_i}$ and $\psi = \sum_{j=1}^m v_j \delta_{y_j}$; and δ_x being the Delta-Dirac function centered on x . Since ϕ and ψ are both probability distributions, sum of weight vectors is 1, $\sum_i u_i = 1 = \sum_j v_j$. The WD distance between



Figure 3: **Example of an intricate image containing multiple similar entities**, and the visual attention map corresponding to the **marked** word in the caption, produced by the GOT module of VoLTA.

ϕ and ψ is defined as:

$$\mathcal{D}_w(\phi, \psi) = \min_{\mathbf{T} \in \Pi(u, v)} \sum \sum \mathbf{T}_{ij} \cdot c(x_i, y_j) \quad (4)$$

where $\Pi(u, v) = \{\mathbf{T} \in \mathbb{R}_+^{n \times m} | \mathbf{T} \mathbf{1}_m = u, \mathbf{T}^\top \mathbf{1}_n = v\}$, $c(x_i, y_j)$ is cosine distance metric, and \mathbf{T} is the transport plan, interpreting the amount of mass shifted from ϕ_i to ψ_j .

Gromov-Wasserstein Distance (GWD) assists in edge matching and preserves graph topology by calculating distances between pairs of nodes in each domain, as well as measuring how these distances compare to the counter domain. In the same discrete graph matching setting, GWD between ϕ and ψ can be mathematically represented as:

$$\mathcal{D}_{gw}(\phi, \psi) = \min_{\hat{\mathbf{T}} \in \Pi(u, v)} \sum_{i, i', j, j'} \hat{\mathbf{T}}_{ij} \hat{\mathbf{T}}_{i'j'} L(x_i, y_j, x'_i, y'_j) \quad (5)$$

where intra-graph structural similarity between two node pairs (x_i, x'_i) and (y_j, y'_j) is represented as $L(x_i, y_j, x'_i, y'_j) = \|c_1(x_i, x'_i) - c_2(y_j, y'_j)\|$, c_i being cosine similarity between a node pair in any graph \mathcal{G}_i . Transport plan $\hat{\mathbf{T}}$ is periodically updated to align the edges in different graphs belonging to disparate modalities.

We further follow Chen et al. (2020a) to combine WD and GWD transport plans, leading to a unified GOT objective given as:

$$\mathcal{L}_{GOT}(\phi, \psi) = \gamma \mathcal{D}_w(\phi, \psi) + (1 - \gamma) \mathcal{D}_{gw}(\phi, \psi) \quad (6)$$

where γ regulates the importance of two loss terms.

3.1.3 CROSS-MODAL ATTENTION FUSION (CMAF)

BT and GOT losses are computed in a dual encoder setting, which does not contain cross-modal interactions and are not suitable for complex multi-modal feature representation. Most existing methods, including UNITER (Chen et al., 2020d), ViLT (Kim et al., 2021), METER (Dou et al., 2022b) and GLIP (Li et al., 2022b) design cross-modal fusion by stacking additional transformer layers on top of uni-modal encoders, introducing large number of added parameters during pre-training. We follow a more efficient solution proposed by FIBER (Dou et al., 2022a), which inserts cross-modal fusion into the uni-modal backbones with a gating mechanism. Specifically, at the top M transformer layers in the vision and language backbone, cross-attention signals, weighted by a gating scalar α , are added to self-attention:

$$\begin{aligned} \hat{x} &= \text{Self-Att}(x) \\ x &= x + \hat{x} + \alpha * \text{Cross-Att}(\hat{x}, y) \\ x &= x + \text{FFN}(x) \end{aligned} \quad (7)$$

where α is a trainable parameter initialized to 0. Following existing literature (Li et al., 2021a; Wang et al., 2021a; Dou et al., 2022b;a), we use Masked Language Modeling (MLM) and Image-Text Matching (ITM) to pre-train the cross-attention parameters. For MLM, we randomly mask 15% text tokens, and the loss aims to reconstruct the masked tokens. We feed the network with randomly sampled image-caption pairs for ITM, and the loss predicts whether they are matched. The gating mechanism is a good choice for CMAF because (i) cross-attention parameters can easily be switched off by setting the gating scalar α to 0 when computing the BT and GOT losses. Thus, we can learn the cross-attention parameters without affecting the original computational flow of uni-modal backbones. (ii) gating mechanism is more lightweight and memory-efficient than adding fusion-specific layers (GLIP and METER use $4 \times$ more fusion parameters than FIBER).

Overall, VoLTA training pipeline can be summarized in the following three steps:

- **BT & GOT:** CMAF is switched off ($\alpha = 0$), VoLTA acts as dual encoder, \mathcal{L}_{BT} and \mathcal{L}_{GOT} are computed.
- **MLM & ITM:** CMAF is switched on ($\alpha \neq 0$), VoLTA now acts as fusion encoder, \mathcal{L}_{MLM} and \mathcal{L}_{ITM} losses are computed.
- **Back-propagation:** the four losses are added, giving $\mathcal{L}_{total} = \mathcal{L}_{BT} + w_{GOT} * \mathcal{L}_{GOT} + \mathcal{L}_{MLM} + \mathcal{L}_{ITM}$, and back-propagated into the model end-to-end. An ablation on w_{GOT} is given in Appendix E.2.

The overall VoLTA pipeline for computation of different training objectives is shown in Figure 2. The pseudo code for VoLTA can be found in Appendix A.

Table 1: **Uni-modal downstream: image classification.** We benchmark learned representations on image classification task by training linear classifiers on fixed features. We report top-1 accuracy on ImageNet-1k validation set, classification mAP on VOC07, and per-class (PC) and overall (O) F1 scores on COCO. Numbers with \dagger are re-implemented by Yuan et al. (2021), and the numbers with \ddagger are re-implemented by us. methods trained with significantly larger dataset are colored gray. Best results are in **bold**.

Linear probing on ImageNet Validation Set					Linear probing on VOC07 and COCO						
Method	Pre-train	Arch.	Supervision	Top-1(%)	Method	Pre-train	Arch.	VOC07		COCO	
								SVM	MLP	MLP (PC/O)	MLP
Sup.	IN-1K	RN50	Label	76.5	Sup.	IN-1K	RN50	87.5	90.8	55.2/60.8	
Sup.	IN-100	RN50	Label	53.3 \dagger	SimCLR	IN-1K	RN50	85.5	—	—	
MoCo	COCO	RN50	NA	44.5 \dagger	MoCo	IN-1K	RN50	79.8	—	—	
MoCo-v2	COCO	RN50	NA	49.3 \dagger	MoCo-v2	IN-1K	RN50	86.4	—	—	
VirTex	COCO	RN50	Caption	52.8	SwAV	IN-1K	RN50	88.9	—	—	
ICMLM	COCO	RN50	Caption	51.9	BYOL	IN-1K	RN50	86.6	—	—	
MCT	COCO	RN50	Caption	54.9	BT	IN-1K	RN50	86.2	91.9 \ddagger	56.1/63.0 \ddagger	
MCT	COCO	RN50	Caption+Tag	55.3	VICReg	IN-1K	RN50	86.6	91.1 \ddagger	51.0/57.9 \ddagger	
VoLTA(w/o CMAF)	COCO	RN50	Caption	55.3	VoLTA(w/o CMAF)	COCO	RN50	89.6	94.3	71.4/74.3	
VoLTA(w/o CMAF)	COCO	Swin-T	Caption	56.3	VoLTA(w/o CMAF)	COCO	Swin-T	88.2	93.5	73.4/75.7	
VoLTA(w/o CMAF)	COCO	Swin-B	Caption	62.5	VoLTA(w/o CMAF)	COCO	Swin-B	88.5	93.9	74.1/76.1	
VoLTA	COCO	Swin-B	Caption	62.5	VoLTA	COCO	Swin-B	88.7	94.0	74.5/76.4	

Table 2: **Uni-modal downstream: object detection and instance segmentation.** We benchmark learned representations on VOC07 + 12 object detection task using faster R-CNN (Ren et al., 2015), and on COCO2017 object detection and instance segmentation using mask R-CNN He et al. (2017), both with C4 backbone variant (Wu et al., 2019). Best results are in **bold**.

Method	Pre-train	Arch.	VOC07+12 det			COCO det			COCO instance seg		
			AP _{all}	AP ₅₀	AP ₇₅	AP ^b ₅₀	AP ^b ₅₀	AP ^b ₇₅	AP ^m ₅₀	AP ^m ₅₀	AP ^m ₇₅
Sup.	IN-1K	RN50	53.5	81.3	58.8	38.2	58.2	41.2	33.3	54.7	35.2
MoCo-v2	IN-1K	RN50	57.4	82.5	64.0	39.3	58.9	42.5	34.4	55.8	36.5
SwAV	IN-1K	RN50	56.1	82.6	62.7	38.4	58.6	41.3	33.8	55.2	35.9
SimSiam	IN-1K	RN50	57.0	82.4	63.7	39.2	59.3	42.1	34.4	56.0	36.7
BT	IN-1K	RN50	56.8	82.6	63.4	39.2	59.0	42.5	34.3	56.0	36.5
MoCo	COCO	RN50	47.5	51.1	75.4	38.5	58.5	42.0	35.0	55.6	37.5
MoCo-v2	COCO	RN50	48.4	52.1	75.5	39.8	59.6	43.1	35.8	56.9	38.8
VirTex	COCO	RN50	55.6	61.5	81.4	40.9	61.7	44.8	36.9	58.4	39.7
MCT	COCO	RN50	56.1	62.4	82.1	41.1	61.8	44.9	36.9	58.2	40.0
VoLTA	COCO	RN50	56.6	62.7	84.4	41.9	61.8	44.8	36.5	58.5	40.8
Sup.	IN-1K	Swin-T	—	—	—	50.5	69.3	54.9	43.7	66.6	47.1
MoBY	IN-1K	Swin-T	—	—	—	50.2	68.8	54.7	43.5	66.1	46.9
VoLTA	COCO	Swin-T	—	—	—	50.9	69.6	55.5	43.8	66.9	47.5
Sup.	IN-1K	Swin-B	—	—	—	51.9	70.9	56.5	45.0	68.4	48.7
VoLTA	COCO	Swin-B	—	—	—	52.1	71.3	56.6	45.2	68.5	49.0

3.2 FINETUNING FOR DOWNSTREAM TASKS

We adopt VoLTA to a wide range of vision- and vision-language downstream tasks. We switch off the inserted cross-attention modules for the vision-only tasks and use the image encoder. For the vision-language tasks, following Dou et al. (2022a), we utilize the learned cross-attention parameters as required. For example, VQA and visual reasoning employ all cross-attention modules, whereas captioning requires only image-to-text cross-attention. Again, during IRTR, we switch off all cross-attentions and use VoLTA in a dual encoder setting. We keep all cross-attention parameters during multi-modal object detection and referring expression comprehension and train an object detection head from scratch using the language-aware image features.

4 EXPERIMENTS

Pre-training & downstream datasets: We pre-train VoLTA on the image-caption pairs of COCO2017 (Lin et al., 2014) split which consists 123k images (118k and 5k for training and validation, respectively) with 5 captions for each image. We divide our downstream tasks into three categories - *(i)* **uni-modal tasks** includes image classification on ImageNet (Deng et al., 2009), VOC07 (Everingham et al., 2010), COCO, object detection on VOC07 + 12, COCO and instance segmentation on COCO. *(ii)* **multi-modal coarse-grained tasks** includes image-level VL tasks - visual question answering on VQAv2 (Antol et al., 2015), visual reasoning on NLVR² (Suhr et al., 2019), image- and text retrieval on Flickr30k (Plummer et al., 2015) and captioning on COCO. *(iii)* **multi-modal fine-grained tasks** includes region-level VL tasks - referring expression comprehension (REC) on RefCOCO, RefCOCO+, RefCOCOg (Kazemzadeh et al., 2014; Yu et al., 2016), and language-conditioned object detection on COCO and LVIS (Gupta et al., 2019). We exclude any overlap between our pre-training and downstream validation/test splits. Detailed statistics of all downstream datasets are given in Appendix C.

Network architectures: Following FIBER (Dou et al., 2022a), we adopt Swin-Base (Liu et al., 2021) and RoBERTa-Base Liu et al. (2019) as our vision and text encoders, which are initialized with weights from uni-modal pre-training. We collect patch- and token features from last transformer

Table 3: **Multi-modal coarse-grained downstreams: visual question answering, visual reasoning, retrieval and captioning.** We only compare with methods pre-trained on comparable amount of dataset. For captioning, 4 metrics are reported - B@4: BLEU@4, M: METEOR, C: CIDEr, S: SPICE. Best comparable results are in **bold**. VoLTA-B denotes Swin-B backbone.

Method	#Pre-train Images	VQAv2		NLVR ²		F30K IRTR		Method	#Pre-train Images	COCO Captioning			
		dev	std	dev	test-P	IR@1	TR@1			B@4	M	C	S
<i>Models pre-trained on COCO (123k) and/or VG (108k)</i>													
SCAN	108k	—	—	—	—	48.6	67.4	VL-T5	180k	34.5	28.7	116.5	21.9
SCG	108k	—	—	—	—	49.3	71.8	VL-BART	180k	35.1	28.7	116.6	21.5
PFAN	108k	—	—	—	—	50.4	70.0	VoLTA-B	123k	37.8	29.9	123.6	22.1
MaxEnt	123k	54.1	54.8	—	—	—	—	VoLTA-GOLD-B	123k	38.4	29.8	126.6	22.4
VisualBERT	123k	70.8	71.0	67.4	67.0	—	—	<i>Models fine-tuned with CIDEr optimization</i>					
LXMERT	231k	72.4	72.5	74.9	74.5	—	—	VoLTA-B	123k	39.4	30.3	132.5	23.3
VoLTA-B	123k	72.8	72.9	69.1	72.9	64.4	78.6	VoLTA-GOLD-B	123k	39.8	30.5	137.5	23.6

layers, and feed them into local projector network to compute GOT loss. Furthermore, we apply AvgPool on patch and token-features, and fed them into global projector network to compute BT loss. Both local and global projector networks has 3 linear layers with dimension 2048-2048-1024, with batch normalization and ReLU after first two layers. An ablation on projector dimension is given in Appendix E.3. During downstream tasks, we use the image and text features after the AvgPool layer. For CMAF, we insert the cross-attention into the top 6 blocks of the vision and text encoders. Moreover, for direct comparison with existing uni-modal baselines, we re-train VoLTA with ResNet50 (He et al., 2016) and Swin-Tiny image encoders.

Implementation details: Detailed implementation setup for pre-training and downstream experiments are given in Appendix D.2 and D.3, respectively.

4.1 RESULTS ON VISION-ONLY TASKS

We first experiment on three uni-modal tasks - classification, object detection, and instance segmentation. For a direct comparison with existing ResNet50 and Swin-T baselines, we re-train identical encoders with VoLTA pipeline. Furthermore, since the uni-modal tasks do not utilize cross-attention parameters, we perform an ablation by dropping the CMAF module from VoLTA.

Image Classification: Table 1 presents the linear probing results of uni-label classification on ImageNet, and multi-label classification on VOC07 and COCO. For ImageNet, we adopt all COCO baselines from Yuan et al. (2021). Even without the CMAF module, VoLTA achieves better performance than all baselines across three datasets with ResNet50 backbone. The Swin backbones and cross-attention module further improve the performance. For VOC07, we report the results for both SVM and MLP-based linear classifiers. VoLTA with ResNet50 backbone achieves state-of-the-art results on VOC07 SVM evaluation, beating the nearest baseline, SwAV, by 0.7 mAP score. These results indicate the ability of VoLTA to learn effective image-level visual features.

Object Detection & Instance Segmentation: Next, we perform two uni-modal region-level tasks - object detection on VOC07 + 12 and COCO2017, and instance segmentation on COCO2017. As shown in Table 2, VoLTA yields the state-of-the-art performance in both tasks across majority metrics. Worth noting, VoLTA, pre-trained with 123k *image-caption* pairs achieves better performance than baselines pre-trained with 1.3M images of ImageNet, proving the efficacy of VLP with fine-grained patch-token alignment over vision-only pre-training.

4.2 RESULTS ON COARSE-GRAINED VISION-LANGUAGE TASKS

Next, we perform image-level multi-modal downstream tasks - visual question answering (VQA), visual reasoning, retrieval, and captioning.

VQA & Visual Reasoning: As reported in Table 3, VoLTA achieves the best performance on VQA and visual reasoning across the baselines pre-trained with a comparable amount of data. Moreover, on VQA, VoLTA beats LXMERT, which is trained with $2 \times$ more data. These results demonstrate the efficacy of our method even when utilizing a mid-scale pre-training corpus.

Retrieval: Most existing VLP methods use a fusion encoder for image and text retrieval and feed every image-text pair into the model. Though such fine-tuning often results in higher performance, it introduces quadratic time-cost and is not scalable. Following Dou et al. (2022a), we adopt a more efficient strategy. We drop the cross-attention parameters for this task and compute the dot product of image and text features extracted separately in the dual-encoder setting. As shown in Table 3, even

Table 4: **Multi-modal fine-grained downstream: referring expression comprehension.** Methods pre-trained on Im-Txt-Box data or significantly larger amount of Im-Txt data are colored gray. Best comparable results are in **bold**. VoLTA-B denotes Swin-B backbone.

Method	#Pre-train Data		RefCOCO			RefCOCO+			RefCOCOg	
	Im-Txt	Im-Txt-Box	val	testA	testB	val	testA	testB	val	test
MAttNet	—	—	76.4	80.4	69.3	64.9	70.3	56.0	66.7	67.0
FAOA	—	—	72.1	74.8	67.6	55.7	60.4	48.5	59.0	58.7
TransVG	—	—	81.0	82.7	78.4	64.8	70.7	56.9	68.7	67.7
ViLBERT	3M	—	—	—	—	72.3	78.5	62.6	—	—
UNITER-L	4M	—	81.4	87.0	74.2	75.9	81.5	66.7	74.9	75.8
VILLA-L	4M	—	82.4	87.5	74.8	76.2	81.5	66.9	76.2	76.7
<i>Models pre-trained on Im-Txt-Box data</i>										
MDETR-B	—	1.3M	87.5	90.4	82.7	81.1	85.5	73.0	83.4	83.3
UniTAB	—	1.3M	86.3	88.8	80.6	78.7	83.2	69.5	80.0	80.0
OFA-L	16M	3M	90.1	92.9	85.3	84.5	90.1	77.8	84.5	85.2
FIBER-B	4M	0.8M	90.7	92.6	87.3	85.7	90.1	79.4	87.1	87.3
VoLTA	123k	—	83.9	86.3	79.4	73.5	78.8	65.5	75.2	75.9

with such an approach, VoLTA produces superior performance among the baselines trained with a similar amount of data, beating all three baselines by a significant margin.

Captioning: We perform captioning on the COCO dataset to evaluate if VoLTA can adopt a generation task. We integrate GOLD (Pang & He, 2021) into VoLTA during fine-tuning as it produces significant improvements. As shown in Table 3, our approach maintains superior captioning performance across all baselines pre-trained with comparable data. Using CIDEr optimization further improves performance.

It is worth mentioning that besides achieving a superior result than all baselines using a comparable amount of data on multi-modal coarse-grained tasks, VoLTA also outperforms multiple methods pre-trained using magnitude more data. These results, shown in Table F.1, indicate the effectiveness and generalizability of VoLTA across these tasks.

4.3 RESULTS ON FINE-GRAINED VISION-LANGUAGE TASKS

Next, we perform region-level multi-modal downstream tasks - referring expression comprehension (REC) and language-guided object detection.

REC: This task aims to localize target objects in an image described by a referring expression phrased in natural language and, thus, perfectly evaluates the fine-grained feature representation capability of VoLTA. As depicted in Table 4, VoLTA beats larger-sized UNITER-L and VILLA-L models on the challenging testB split of both RefCOCO and RefCOCO+. Moreover, VoLTA performs comparably with MDETR and UniTAB, even without being trained on grounding data. These results indicate our model’s efficacy in learning fine-grained local visual features.

Object Detection: We evaluate VoLTA on two challenging language-conditioned object detection benchmarks - COCO and LVIS. Note that, all existing baselines for this tasks are pre-trained on fine-grained *image-text-box* data, whereas VoLTA only utilizes *image-caption* pairs. As shown in Table 5, VoLTA performs comparatively with these strong baselines. Note that VoLTA beats Mask R-CNN, MDETR, and GLIP-B on LVIS APr, which denotes average precision on rare objects. Thus, we conclude that VoLTA achieves impressive localization ability and robustness, even without utilizing any grounding annotations.

5 CONCLUSION

We present VoLTA, a unified VLP paradigm that utilizes image-caption data but achieves fine-grained region-level image understanding, eliminating the use of expensive box annotations. VoLTA adopts graph optimal transport-based weakly supervised patch-token alignment and produces an explicit,

Table 5: **Multi-modal fine-grained downstream: language-conditioned object detection on COCO and LVIS.** All available baselines are pre-trained on Im-Txt-Box data, and are colored gray. VoLTA-B denotes Swin-B backbone.

Method	COCO Val 2017		LVIS MiniVal			
	AP	APr	APc	APf	AP	AP
<i>Models pre-trained on Im-Txt-Box and/or with larger size</i>						
Mask R-CNN	—	—	26.3	34.0	33.9	33.3
MDETR	—	—	20.9	24.9	24.3	24.2
GLIP-B	57.0	—	31.3	48.3	56.9	51.0
GLIP-L	60.8	—	—	—	—	—
FIBER-B	58.4	—	50.0	56.9	58.1	56.9
VoLTA	50.9	32.3	42.2	42.9	41.7	—

self-normalized, and interpretable low-level matching criterion. Extensive experiments demonstrate the effectiveness of VoLTA on a wide range of coarse- and fine-grained tasks. In the future, we plan to pre-train VoLTA on larger-scale datasets.

REPRODUCIBILITY STATEMENT

The pre-training code of VoLTA can be found in the supplementary material. We also provide a detailed implementation setup for pre-training and downstream experiments in Appendix D.2 and D.3, respectively. After publication, we will provide pre-trained checkpoints and open-source the code on a public repository.

REFERENCES

Peter Anderson, Basura Fernando, Mark Johnson, and Stephen Gould. Spice: Semantic propositional image caption evaluation. In *European conference on computer vision*, pp. 382–398. Springer, 2016.

Stanislaw Antol, Aishwarya Agrawal, Jiasen Lu, Margaret Mitchell, Dhruv Batra, C Lawrence Zitnick, and Devi Parikh. Vqa: Visual question answering. In *Proceedings of the IEEE international conference on computer vision*, pp. 2425–2433, 2015.

Mahmoud Assran, Mathilde Caron, Ishan Misra, Piotr Bojanowski, Florian Bordes, Pascal Vincent, Armand Joulin, Michael G. Rabbat, and Nicolas Ballas. Masked siamese networks for label-efficient learning. *ArXiv*, abs/2204.07141, 2022.

Yogesh Balaji, Rama Chellappa, and Soheil Feizi. Normalized wasserstein for mixture distributions with applications in adversarial learning and domain adaptation. In *Proceedings of the IEEE/CVF International Conference on Computer Vision*, pp. 6500–6508, 2019.

Satanjeev Banerjee and Alon Lavie. Meteor: An automatic metric for mt evaluation with improved correlation with human judgments. In *Proceedings of the acl workshop on intrinsic and extrinsic evaluation measures for machine translation and/or summarization*, pp. 65–72, 2005.

Hangbo Bao, Li Dong, Songhao Piao, and Furu Wei. Beit: Bert pre-training of image transformers. In *International Conference on Learning Representations*, 2021.

Adrien Bardes, Jean Ponce, and Yann LeCun. Vicreg: Variance-invariance-covariance regularization for self-supervised learning. In *International Conference on Learning Representations*, 2022.

Tom Brown, Benjamin Mann, Nick Ryder, Melanie Subbiah, Jared D Kaplan, Prafulla Dhariwal, Arvind Neelakantan, Pranav Shyam, Girish Sastry, Amanda Askell, et al. Language models are few-shot learners. *Advances in neural information processing systems*, 33:1877–1901, 2020.

Mathilde Caron, Hugo Touvron, Ishan Misra, Herv'e J'egou, Julien Mairal, Piotr Bojanowski, and Armand Joulin. Emerging properties in self-supervised vision transformers. *2021 IEEE/CVF International Conference on Computer Vision (ICCV)*, pp. 9630–9640, 2021.

Chun-Fu (Richard) Chen, Quanfu Fan, and Rameswar Panda. CrossViT: Cross-Attention Multi-Scale Vision Transformer for Image Classification. In *International Conference on Computer Vision (ICCV)*, 2021a.

Liqun Chen, Yizhe Zhang, Ruiyi Zhang, Chenyang Tao, Zhe Gan, Haichao Zhang, Bai Li, Dinghan Shen, Changyou Chen, and Lawrence Carin. Improving sequence-to-sequence learning via optimal transport. In *International Conference on Learning Representations*, 2019. URL <https://openreview.net/forum?id=S1xtAjR5tX>.

Liqun Chen, Zhe Gan, Yu Cheng, Linjie Li, Lawrence Carin, and Jingjing Liu. Graph optimal transport for cross-domain alignment. In *International Conference on Machine Learning*, pp. 1542–1553. PMLR, 2020a.

Ting Chen, Simon Kornblith, Mohammad Norouzi, and Geoffrey Hinton. A simple framework for contrastive learning of visual representations. In *International conference on machine learning*, pp. 1597–1607. PMLR, 2020b.

Xinlei Chen and Kaiming He. Exploring simple siamese representation learning. *2021 IEEE/CVF Conference on Computer Vision and Pattern Recognition (CVPR)*, pp. 15745–15753, 2021.

Xinlei Chen, Haoqi Fan, Ross Girshick, and Kaiming He. Improved baselines with momentum contrastive learning. *arXiv preprint arXiv:2003.04297*, 2020c.

Xinlei Chen, Saining Xie, and Kaiming He. An empirical study of training self-supervised vision transformers. *2021 IEEE/CVF International Conference on Computer Vision (ICCV)*, pp. 9620–9629, 2021b.

Yen-Chun Chen, Linjie Li, Licheng Yu, Ahmed El Kholy, Faisal Ahmed, Zhe Gan, Yu Cheng, and Jingjing Liu. Uniter: Universal image-text representation learning. In *European conference on computer vision*, pp. 104–120. Springer, 2020d.

Jaemin Cho, Jie Lei, Hao Tan, and Mohit Bansal. Unifying vision-and-language tasks via text generation. In *International Conference on Machine Learning*, pp. 1931–1942. PMLR, 2021.

Jia Deng, Wei Dong, Richard Socher, Li-Jia Li, Kai Li, and Li Fei-Fei. Imagenet: A large-scale hierarchical image database. In *2009 IEEE conference on computer vision and pattern recognition*, pp. 248–255. Ieee, 2009.

Jacob Devlin, Ming-Wei Chang, Kenton Lee, and Kristina Toutanova. Bert: Pre-training of deep bidirectional transformers for language understanding. In *Proceedings of the 2019 Conference of the North American Chapter of the Association for Computational Linguistics: Human Language Technologies, Volume 1 (Long and Short Papers)*, pp. 4171–4186, 2019.

Alexey Dosovitskiy, Lucas Beyer, Alexander Kolesnikov, Dirk Weissenborn, Xiaohua Zhai, Thomas Unterthiner, Mostafa Dehghani, Matthias Minderer, Georg Heigold, Sylvain Gelly, Jakob Uszkoreit, and Neil Houlsby. An image is worth 16x16 words: Transformers for image recognition at scale. In *International Conference on Learning Representations*, 2021. URL <https://openreview.net/forum?id=YicbFdNTTy>.

Zi-Yi Dou, Aishwarya Kamath, Zhe Gan, Pengchuan Zhang, Jianfeng Wang, Linjie Li, Zicheng Liu, Ce Liu, Yann LeCun, Nanyun Peng, et al. Coarse-to-fine vision-language pre-training with fusion in the backbone. *Advances in neural information processing systems*, 2022a.

Zi-Yi Dou, Yichong Xu, Zhe Gan, Jianfeng Wang, Shuohang Wang, Lijuan Wang, Chenguang Zhu, Pengchuan Zhang, Lu Yuan, Nanyun Peng, et al. An empirical study of training end-to-end vision-and-language transformers. In *Proceedings of the IEEE/CVF Conference on Computer Vision and Pattern Recognition*, pp. 18166–18176, 2022b.

Mark Everingham, Luc Van Gool, Christopher KI Williams, John Winn, and Andrew Zisserman. The pascal visual object classes (voc) challenge. *International journal of computer vision*, 88(2):303–338, 2010.

Tianyu Gao, Xingcheng Yao, and Danqi Chen. Simcse: Simple contrastive learning of sentence embeddings. In *Proceedings of the 2021 Conference on Empirical Methods in Natural Language Processing*, pp. 6894–6910, 2021.

Quentin Garrido, Yubei Chen, Adrien Bardes, Laurent Najman, and Yann Lecun. On the duality between contrastive and non-contrastive self-supervised learning. *arXiv preprint arXiv:2206.02574*, 2022.

Aude Genevay, Gabriel Peyré, and Marco Cuturi. Learning generative models with sinkhorn divergences. In *International Conference on Artificial Intelligence and Statistics*, pp. 1608–1617. PMLR, 2018.

Xinyang Geng, Hao Liu, Lisa Lee, Dale Schuurmans, Sergey Levine, and P. Abbeel. Multimodal masked autoencoders learn transferable representations. *ArXiv*, abs/2205.14204, 2022.

Priya Goyal, Piotr Dollár, Ross Girshick, Pieter Noordhuis, Lukasz Wesolowski, Aapo Kyrola, Andrew Tulloch, Yangqing Jia, and Kaiming He. Accurate, large minibatch sgd: Training imagenet in 1 hour. *arXiv preprint arXiv:1706.02677*, 2017.

Jean-Bastien Grill, Florian Strub, Florent Altché, Corentin Tallec, Pierre Richemond, Elena Buchatskaya, Carl Doersch, Bernardo Avila Pires, Zhaohan Guo, Mohammad Gheshlaghi Azar, et al. Bootstrap your own latent-a new approach to self-supervised learning. *Advances in neural information processing systems*, 33:21271–21284, 2020.

Agrim Gupta, Piotr Dollar, and Ross Girshick. Lvis: A dataset for large vocabulary instance segmentation. In *Proceedings of the IEEE/CVF conference on computer vision and pattern recognition*, pp. 5356–5364, 2019.

Song Han, Jeff Pool, John Tran, and William Dally. Learning both weights and connections for efficient neural network. *Advances in neural information processing systems*, 28, 2015.

Kaiming He, Xiangyu Zhang, Shaoqing Ren, and Jian Sun. Deep residual learning for image recognition. In *Proceedings of the IEEE conference on computer vision and pattern recognition*, pp. 770–778, 2016.

Kaiming He, Georgia Gkioxari, Piotr Dollár, and Ross Girshick. Mask r-cnn. In *Proceedings of the IEEE international conference on computer vision*, pp. 2961–2969, 2017.

Kaiming He, Haoqi Fan, Yuxin Wu, Saining Xie, and Ross Girshick. Momentum contrast for unsupervised visual representation learning. In *Proceedings of the IEEE/CVF conference on computer vision and pattern recognition*, pp. 9729–9738, 2020.

Kaiming He, Xinlei Chen, Saining Xie, Yanghao Li, Piotr Dollár, and Ross Girshick. Masked autoencoders are scalable vision learners. In *Proceedings of the IEEE/CVF Conference on Computer Vision and Pattern Recognition*, pp. 16000–16009, 2022.

Zhicheng Huang, Zhaoyang Zeng, Bei Liu, Dongmei Fu, and Jianlong Fu. Pixel-bert: Aligning image pixels with text by deep multi-modal transformers. *arXiv preprint arXiv:2004.00849*, 2020.

Zhicheng Huang, Zhaoyang Zeng, Yupan Huang, Bei Liu, Dongmei Fu, and Jianlong Fu. Seeing out of the box: End-to-end pre-training for vision-language representation learning. In *Proceedings of the IEEE/CVF Conference on Computer Vision and Pattern Recognition*, pp. 12976–12985, 2021.

Chao Jia, Yinfei Yang, Ye Xia, Yi-Ting Chen, Zarana Parekh, Hieu Pham, Quoc Le, Yun-Hsuan Sung, Zhen Li, and Tom Duerig. Scaling up visual and vision-language representation learning with noisy text supervision. In *International Conference on Machine Learning*, pp. 4904–4916. PMLR, 2021.

Aishwarya Kamath, Mannat Singh, Yann LeCun, Gabriel Synnaeve, Ishan Misra, and Nicolas Carion. Mdetr-modulated detection for end-to-end multi-modal understanding. In *Proceedings of the IEEE/CVF International Conference on Computer Vision*, pp. 1780–1790, 2021.

Sahar Kazemzadeh, Vicente Ordonez, Mark Matten, and Tamara Berg. Referitgame: Referring to objects in photographs of natural scenes. In *Proceedings of the 2014 conference on empirical methods in natural language processing (EMNLP)*, pp. 787–798, 2014.

Douwe Kiela, Suvat Bhooshan, Hamed Firooz, and Davide Testuggine. Supervised multimodal bitransformers for classifying images and text. *ArXiv*, abs/1909.02950, 2019.

Wonjae Kim, Bokyoung Son, and Ildoo Kim. Vilt: Vision-and-language transformer without convolution or region supervision. In *International Conference on Machine Learning*, pp. 5583–5594. PMLR, 2021.

Junnan Li, Ramprasaath Selvaraju, Akhilesh Gotmare, Shafiq Joty, Caiming Xiong, and Steven Chu Hong Hoi. Align before fuse: Vision and language representation learning with momentum distillation. *Advances in neural information processing systems*, 34:9694–9705, 2021a.

Junnan Li, Dongxu Li, Caiming Xiong, and Steven Hoi. Blip: Bootstrapping language-image pre-training for unified vision-language understanding and generation. In *International Conference on Machine Learning*, 2022a.

Liunian Harold Li, Mark Yatskar, Da Yin, Cho-Jui Hsieh, and Kai-Wei Chang. What does bert with vision look at? In *Proceedings of the 58th Annual Meeting of the Association for Computational Linguistics*, pp. 5265–5275, 2020a.

Liunian Harold Li, Pengchuan Zhang, Haotian Zhang, Jianwei Yang, Chunyuan Li, Yiwu Zhong, Lijuan Wang, Lu Yuan, Lei Zhang, Jenq-Neng Hwang, et al. Grounded language-image pre-training. In *Proceedings of the IEEE/CVF Conference on Computer Vision and Pattern Recognition*, pp. 10965–10975, 2022b.

Manling Li, Ruochen Xu, Shuohang Wang, Luowei Zhou, Xudong Lin, Chenguang Zhu, Michael Zeng, Heng Ji, and Shih-Fu Chang. Clip-event: Connecting text and images with event structures. In *Proceedings of the IEEE/CVF Conference on Computer Vision and Pattern Recognition*, pp. 16420–16429, 2022c.

Xiujun Li, Xi Yin, Chunyuan Li, Pengchuan Zhang, Xiaowei Hu, Lei Zhang, Lijuan Wang, Houdong Hu, Li Dong, Furu Wei, et al. Oscar: Object-semantics aligned pre-training for vision-language tasks. In *European Conference on Computer Vision*, pp. 121–137. Springer, 2020b.

Yangguang Li, Feng Liang, Lichen Zhao, Yufeng Cui, Wanli Ouyang, Jing Shao, Fengwei Yu, and Junjie Yan. Supervision exists everywhere: A data efficient contrastive language-image pre-training paradigm. In *International Conference on Learning Representations*, 2021b.

Yujia Li, Chenjie Gu, Thomas Dullien, Oriol Vinyals, and Pushmeet Kohli. Graph matching networks for learning the similarity of graph structured objects. In *International conference on machine learning*, pp. 3835–3845. PMLR, 2019.

Tsung-Yi Lin, Michael Maire, Serge Belongie, James Hays, Pietro Perona, Deva Ramanan, Piotr Dollár, and C Lawrence Zitnick. Microsoft coco: Common objects in context. In *European conference on computer vision*, pp. 740–755. Springer, 2014.

Yinhan Liu, Myle Ott, Naman Goyal, Jingfei Du, Mandar Joshi, Danqi Chen, Omer Levy, Mike Lewis, Luke Zettlemoyer, and Veselin Stoyanov. Roberta: A robustly optimized bert pretraining approach. *arXiv preprint arXiv:1907.11692*, 2019.

Ze Liu, Yutong Lin, Yue Cao, Han Hu, Yixuan Wei, Zheng Zhang, Stephen Lin, and Baining Guo. Swin transformer: Hierarchical vision transformer using shifted windows. In *Proceedings of the IEEE/CVF International Conference on Computer Vision*, pp. 10012–10022, 2021.

Jiasen Lu, Dhruv Batra, Devi Parikh, and Stefan Lee. Vilbert: Pretraining task-agnostic visiolinguistic representations for vision-and-language tasks. *Advances in neural information processing systems*, 32, 2019.

Youssef Mroueh, Chun-Liang Li, Tom Sercu, Anant Raj, and Yu Cheng. Sobolev gan. In *International Conference on Learning Representations*, 2018.

Youssef Mroueh, Tom Sercu, and Anant Raj. Sobolev descent. In *The 22nd International Conference on Artificial Intelligence and Statistics*, pp. 2976–2985. PMLR, 2019.

Norman Mu, Alexander Kirillov, David A. Wagner, and Saining Xie. Slip: Self-supervision meets language-image pre-training. *ArXiv*, abs/2112.12750, 2021.

Aaron van den Oord, Yazhe Li, and Oriol Vinyals. Representation learning with contrastive predictive coding. *arXiv preprint arXiv:1807.03748*, 2018.

Richard Yuanzhe Pang and He He. Text generation by learning from demonstrations. In *ICLR*, 2021.

Kishore Papineni, Salim Roukos, Todd Ward, and Wei-Jing Zhu. Bleu: a method for automatic evaluation of machine translation. In *Proceedings of the 40th annual meeting of the Association for Computational Linguistics*, pp. 311–318, 2002.

Gabriel Peyré, Marco Cuturi, and Justin Solomon. Gromov-wasserstein averaging of kernel and distance matrices. In *International Conference on Machine Learning*, pp. 2664–2672. PMLR, 2016.

Gabriel Peyré, Marco Cuturi, et al. Computational optimal transport: With applications to data science. *Foundations and Trends® in Machine Learning*, 11(5-6):355–607, 2019.

Bryan A Plummer, Liwei Wang, Chris M Cervantes, Juan C Caicedo, Julia Hockenmaier, and Svetlana Lazebnik. Flickr30k entities: Collecting region-to-phrase correspondences for richer image-to-sentence models. In *Proceedings of the IEEE international conference on computer vision*, pp. 2641–2649, 2015.

Shraman Pramanick, Aniket Roy, and Vishal M Patel. Multimodal learning using optimal transport for sarcasm and humor detection. In *Proceedings of the IEEE/CVF Winter Conference on Applications of Computer Vision*, pp. 3930–3940, 2022.

Alec Radford, Jeff Wu, Rewon Child, David Luan, Dario Amodei, and Ilya Sutskever. Language models are unsupervised multitask learners. 2019.

Alec Radford, Jong Wook Kim, Chris Hallacy, Aditya Ramesh, Gabriel Goh, Sandhini Agarwal, Girish Sastry, Amanda Askell, Pamela Mishkin, Jack Clark, et al. Learning transferable visual models from natural language supervision. In *International Conference on Machine Learning*, pp. 8748–8763. PMLR, 2021.

Shaoqing Ren, Kaiming He, Ross Girshick, and Jian Sun. Faster r-cnn: Towards real-time object detection with region proposal networks. *Advances in neural information processing systems*, 28, 2015.

Amanpreet Singh, Ronghang Hu, Vedanuj Goswami, Guillaume Couairon, Wojciech Galuba, Marcus Rohrbach, and Douwe Kiela. Flava: A foundational language and vision alignment model. In *Proceedings of the IEEE/CVF Conference on Computer Vision and Pattern Recognition*, pp. 15638–15650, 2022.

Weijie Su, Xizhou Zhu, Yue Cao, Bin Li, Lewei Lu, Furu Wei, and Jifeng Dai. Vi-bert: Pre-training of generic visual-linguistic representations. In *International Conference on Learning Representations*, 2019.

Alane Suhr, Stephanie Zhou, Ally Zhang, Iris Zhang, Huajun Bai, and Yoav Artzi. A corpus for reasoning about natural language grounded in photographs. In *Proceedings of the Annual Meeting of the Association for Computational Linguistics*, 2019.

Hao Tan and Mohit Bansal. Lxmert: Learning cross-modality encoder representations from transformers. In *Proceedings of the 2019 Conference on Empirical Methods in Natural Language Processing and the 9th International Joint Conference on Natural Language Processing (EMNLP-IJCNLP)*, pp. 5100–5111, 2019.

Ramakrishna Vedantam, C Lawrence Zitnick, and Devi Parikh. Cider: Consensus-based image description evaluation. In *Proceedings of the IEEE conference on computer vision and pattern recognition*, pp. 4566–4575, 2015.

Peng Wang, An Yang, Rui Men, Junyang Lin, Shuai Bai, Zhikang Li, Jianxin Ma, Chang Zhou, Jingren Zhou, and Hongxia Yang. Ofa: Unifying architectures, tasks, and modalities through a simple sequence-to-sequence learning framework. In *International Conference on Machine Learning*, pp. 23318–23340. PMLR, 2022a.

Wenhui Wang, Hangbo Bao, Li Dong, and Furu Wei. Vlmo: Unified vision-language pre-training with mixture-of-modality-experts. *arXiv preprint arXiv:2111.02358*, 2021a.

Wenhui Wang, Hangbo Bao, Li Dong, Johan Bjorck, Zhiliang Peng, Qiang Liu, Kriti Aggarwal, Owais Mohammed, Saksham Singhal, Subhrojot Som, and Furu Wei. Image as a foreign language: Beit pretraining for all vision and vision-language tasks. *ArXiv*, abs/2208.10442, 2022b.

Zirui Wang, Jiahui Yu, Adams Wei Yu, Zihang Dai, Yulia Tsvetkov, and Yuan Cao. Simvlm: Simple visual language model pretraining with weak supervision. In *International Conference on Learning Representations*, 2021b.

Jason Wei and Kai Zou. Eda: Easy data augmentation techniques for boosting performance on text classification tasks. In *Proceedings of the 2019 Conference on Empirical Methods in Natural Language Processing and the 9th International Joint Conference on Natural Language Processing (EMNLP-IJCNLP)*, pp. 6382–6388, 2019.

Yuxin Wu, Alexander Kirillov, Francisco Massa, Wan-Yen Lo, and Ross Girshick. Detectron2. <https://github.com/facebookresearch/detectron2>, 2019.

Hongwei Xue, Yupan Huang, Bei Liu, Houwen Peng, Jianlong Fu, Houqiang Li, and Jiebo Luo. Probing inter-modality: Visual parsing with self-attention for vision-and-language pre-training. *Advances in Neural Information Processing Systems*, 34:4514–4528, 2021.

Jianwei Yang, Chunyuan Li, Pengchuan Zhang, Bin Xiao, Ce Liu, Lu Yuan, and Jianfeng Gao. Unified contrastive learning in image-text-label space. In *Proceedings of the IEEE/CVF Conference on Computer Vision and Pattern Recognition*, pp. 19163–19173, 2022a.

Zhengyuan Yang, Zhe Gan, Jianfeng Wang, Xiaowei Hu, Faisal Ahmed, Zicheng Liu, Yumao Lu, and Lijuan Wang. Unitab: Unifying text and box outputs for grounded vision-language modeling. In *ECCV*, 2022b.

Yang You, Igor Gitman, and Boris Ginsburg. Large batch training of convolutional networks. *arXiv preprint arXiv:1708.03888*, 2017.

Licheng Yu, Patrick Poirson, Shan Yang, Alexander C Berg, and Tamara L Berg. Modeling context in referring expressions. In *European Conference on Computer Vision*, pp. 69–85. Springer, 2016.

Siyang Yuan, Ke Bai, Liqun Chen, Yizhe Zhang, Chenyang Tao, Chunyuan Li, Guoyin Wang, Ricardo Henao, and Lawrence Carin. Advancing weakly supervised cross-domain alignment with optimal transport. In *BMVC*, 2020.

Xin Yuan, Zhe Lin, Jason Kuen, Jianming Zhang, Yilin Wang, Michael Maire, Ajinkya Kale, and Baldo Faieta. Multimodal contrastive training for visual representation learning. In *Proceedings of the IEEE/CVF Conference on Computer Vision and Pattern Recognition*, pp. 6995–7004, 2021.

Jure Zbontar, Li Jing, Ishan Misra, Yann LeCun, and Stéphane Deny. Barlow twins: Self-supervised learning via redundancy reduction. In *International Conference on Machine Learning*, pp. 12310–12320. PMLR, 2021.

Chi Zhang, Yujun Cai, Guosheng Lin, and Chunhua Shen. Deepemd: Few-shot image classification with differentiable earth mover’s distance and structured classifiers. In *Proceedings of the IEEE/CVF conference on computer vision and pattern recognition*, pp. 12203–12213, 2020.

Haotian Zhang, Pengchuan Zhang, Xiaowei Hu, Yen-Chun Chen, Liunian Harold Li, Xiyang Dai, Lijuan Wang, Lu Yuan, Jenq-Neng Hwang, and Jianfeng Gao. Glipv2: Unifying localization and vision-language understanding. *Advances in Neural Information Processing Systems*, 2022.

Pengchuan Zhang, Xiuju Li, Xiaowei Hu, Jianwei Yang, Lei Zhang, Lijuan Wang, Yejin Choi, and Jianfeng Gao. Vinvl: Revisiting visual representations in vision-language models. In *Proceedings of the IEEE/CVF Conference on Computer Vision and Pattern Recognition*, pp. 5579–5588, 2021.

A PESUDO CODE OF VOLTA

The training psuedo code for VoLTA is as follows:

Algorithm 1 PyTorch-style pseudocode for VoLTA.

```
# f_I: Image Encoder, f_T: Text Encoder
# task_names: string containing task names
# I: Image input, T: Text input, N: Batch size, D: Projector dim
# BT: Barlow Twins loss function
# WD, GWD: Wasserstein and Gromov-Wasserstein loss functions
# MLM, ITM: MLM and ITM loss functions, respectively
# gamma: coefficient of GWD loss in GOT
# w_GOT: weight of GOT loss

def GOT(x_1, x_2, f_1, f_2):
    # compute embeddings
    z_A, z_B = f_1(x_1), f_2(x_2) # N x D

    # normalize representation along batch dimension
    z_A_norm = (z_A - z_A.mean(dim=0)) / z_A.std(dim=0)
    z_B_norm = (z_B - z_B.mean(dim=0)) / z_B.std(dim=0)

    # cosine distance matrix
    c = cosine_dist_matrix(z_A, z_B)
    # Wasserstein distance
    loss_w = W_D(c, z_A.size(0), z_A.size(1), z_B.size(1))
    # Gromov-Wasserstein distance
    loss_gw = GW_D(z_A.transpose(2,1), z_B.transpose(2,1))

    return gamma * torch.mean(loss_gw) + (1 - gamma) * torch.mean(loss_w)

def VoLTA (I, T):
    total_loss = torch.tensor(0.)
    for x in loader: # load a batch with N samples
        # two augmented versions of I, T
        I1, I2 = augment_image(I); T1, T2 = augment_text(T)

        if "BTGOT" in task_names:
            # BT loss
            intra_loss = BT(I1, I2, f_I) + BT(T1, T2, f_T)
            inter_loss = BT(I1, T1, f_I, f_T) + BT(I2, T2, f_I, f_T)
            BT_loss = intra_loss + inter_loss
            total_loss += BT_loss

            # GOT loss
            GOT_loss = GOT(I1, T1, f_I, f_T) + GOT(I2, T2, f_I, f_T)
            total_loss += w_GOT * GOT_loss

        # cross-attention is enabled
        if "MLM" in task_names:

            # MLM loss
            MLM_loss = MLM(T1, I1, mask_T1, f_I, f_T)
            total_loss += MLM_loss

        if "ITM" in task_names:

            # ITM loss
            ITM_loss = ITM(T1, I1, false_image_1, f_I, f_T)
            total_loss += ITM_loss

    return total_loss
```

Table B.1: **Overview of VLP models.** OD: objective detector. Xformer: transformer. Emb.: embedding. MLM/MIM: masked language/image modeling. ITM: image-text matching. WRA: word-region alignment. ITC: image-text contrastive learning. Grnd: Grounding. Cap: Captioning. TP: Token Prediction. CA: Contrastive Alignment, NNS: Nearest Neighbour Supervision, MVS: Multiview Supervision, SL: Sim-siam Loss, MHA: Multi-head attn. LM: Language Modeling, I-T: Image-Text, I-T-B: Image-Text-Box.

Model	Venue	Vision Encoder	Text Enc.	Multity Fusion	Pre-train I-T	Pre-train I-T-B	Pre-training Objectives
ViLBERT	NeurIPS'19	OD+Xformer	Xformer	Co-attn.	✓		MLM+ITM+MIM
LXMERT	EMNLP'19				✓		MLM+ITM+MIM+VQA
VisualBERT	ACL'20				✓		MLM+ITM
VL-BERT	ICLR'20				✓		MLM+MIM
UNITER	ECCV'20				✓		MLM+ITM+MIM+WRA
OSCAR	ECCV'20				✓		MLM+ITM
VinVL	CVPR'21				✓		MLM+ITM
VL-T5	ICML'21					✓	MLM+ITM+VQA+Grnd+Cap
SOHO	CVPR'21				✓		MLM+ITM+MIM
SimVLM	ICLR'22	CNN	Emb.	Merged-attn.			PrefixLM
MDETR	ICCV'21		Xformer			✓	OD+TP+CA
ViLT	ICML'21	Patch Emb.		Merged-attn.	✓		MLM+ITM
Visual Parsing	NeurIPS'21		Emb.		✓		MLM+ITM+MIM
ALBEF	NeurIPS'21				✓		MLM+ITM+ITC
METER	CVPR'22	Xformer		Co-attn.	✓		MLM+ITM
CLIP	ICML'21	CNN/Xformer		None	✓		ITC
DeCLIP	ICLR'21				✓		ITC+MLM+SL+MVS+NNS
ALIGN	ICML'21	CNN			✓		ITC
GLIP	CVPR'22		Xformer	Cross-modality MHA	✓	✓	OD+CE+WRA
GLIPv2	NeurIPS'22	OD+Xformer			✓	✓	OD+CE+WRA+MLM
BLIP	ICML'22	Xformer			✓		ITC+ITM+LM
UniCL	CVPR'22	CNN/Xformer		None	✓		ITC
UniTAB	ECCV'22	CNN		Merged Attn		✓	LM
FIBER	NeurIPS'22	Xformer	Xformer	Merged Co-attn	✓	✓	MLM+ITM+ITC
VoLTA	—	CNN/Xformer	Xformer	Merged Co-attn	✓		BT+GOT+MLM+ITM

B OVERVIEW OF VISION-LANGUAGE PRE-TRAINING MODELS

Vision-Language Pretrained (VLP) models have proven extremely beneficial for multi-modal tasks in recent years. Earlier works were predominantly focused on using pre-trained object detectors to extract patch (region) level information from corresponding images (Lu et al., 2019; Li et al., 2020a; Tan & Bansal, 2019; Chen et al., 2020d; Su et al., 2019). In some of these models, such as ViLBERT (Lu et al., 2019) and LXMERT (Tan & Bansal, 2019), multi-modality fusion has been achieved via co-attention which utilizes a third transformer that contains fused information independently obtained from respective vision and language encoders (transformer). On the contrary, VisualBERT (Li et al., 2020a), VL-BERT (Su et al., 2019) and UNITER (Chen et al., 2020d) employ a merged attention strategy to fuse both image patches and text features together into a unified transformer through corresponding image and text embedders. In addition to image patches and texts in a unified transformer, OSCAR (Li et al., 2020b) uses object tags as inputs. VinVL (Zhang et al., 2021) follows a similar strategy to that of OSCAR, the only difference being their novel 3-way contrastive loss which optimizes the training objectives used for VQA and text-image matching. VL-T5 (Cho et al., 2021) exploits bounding-box coordinate information, image IDs, and region IDs along with ROI features for visual embedding. Encoded visual and textual features are fed into a bi-directional multi-modal encoder and an auto-regressive text decoder framework for pre-training.

In all the methods mentioned above, pre-trained object detectors are usually frozen during the training, and extracting region-level features from images can be tedious. To address these shortcomings, end-to-end pre-training methods have been developed. PixelBERT (Huang et al., 2020) uses convolutional neural networks (CNNs) based visual encoder and sentence encoder to obtain image and text representations, respectively, fed to a subsequent transformer via a cross-modality alignment. SOHO (Huang et al., 2021) uses grid features discretization via a learned vision dictionary which are then fed into a cross-modal module. SimVLM (Wang et al., 2021b) uses CNN and text token embedding for image and text feature representation extraction along with a unified encoder-decoder transformer trained on a PrefixLM objective. Finally, MDETR (Kamath et al., 2021) uses CNN and RoBERTa (along with corresponding projection layers) for image and text feature extraction, which are then concatenated before passing through a unified transformer trained on 1.3M Image-Text-Box (I-T-B) annotated data.

Table C.1: **Dataset statistics for uni-modal and multi-modal downstream tasks.**

Modality	Task	Dataset	Image Src	#Images	#Text	Metric
Uni-modal	Image Classfn.	IN-1K	IN-1K	1.3M	-	Accuracy
		COCO	COCO	123K	-	F1
		VOC07+12	VOC07+12	16K	-	mAP
	Object Det.	COCO	COCO	123K	-	AP ^{bb}
		VOC07+12	VOC07+12	16K	-	AP ^{mk}
	Instance Seg.	COCO	COCO	123K	-	AP ^{mk}
Multi-modal coarse-grained	VQA	VQA	COCO	204K	1.1M	VQA-Score
	NLVR ²	NLVR ²	Web Crawled	214K	107K	Accuracy
	IR-TR	Flickr30K	Flickr30K	32K	160K	Recall@1
	Captioning	COCO	COCO	123K	615K	B@4,M,C,S
Multi-modal fine-grained	Ref. Exp. Comp.	RefCOCO+	COCO	20K	142K	Accuracy
		RefCOCOg	COCO	26K	95K	
	Mul. Obj. Det.	COCO	COCO	123K	615K	AP
		LVIS Mini	COCO	123K	615K	

In recent years, the rise of Vision Transformers (ViT) (Dosovitskiy et al., 2021) has motivated the research community to have an all-transformer framework by incorporating ViTs (instead of CNN backbones) in VLP models. Image patch features and text token embeddings are fed directly into a ViT model for pre-training in VILT (Kim et al., 2021). Visual Parsing (Xue et al., 2021), ALBEF (Li et al., 2021a) and METER (Dou et al., 2022b) use ViTs as vision encoders for image feature generation. For multimodal fusion, ALBEF and METER use co-attention in their pre-training frameworks.

Another class of VLP models in the form of CLIP (Radford et al., 2021), DeCLIP (Li et al., 2021b) and ALIGN (Jia et al., 2021) have been introduced lately. Although, known for their impressive zero-shot recognition ability and excellent transferability to downstream tasks, these models typically rely on huge amount of image-text pairs for pre-training. Contrastive loss forms the core component of the pre-training objectives in these VLP models. GLIP (Li et al., 2022b) and GLIPv2 (Zhang et al., 2022) use a localization loss along with a word-region alignment loss for pre-training corresponding encoders using image-text-box annotations. BLIP (Li et al., 2022a) employs image and text encoders connected through a cross-modality multi-head attention which are pre-trained on image-text pairs using contrastive and language modeling objectives. UniCL (Yang et al., 2022a) utilizes a unified learning method with a two-way contrastive loss (image-to-text and text-to-image) in the image-text-label space which can learn representations from either of the image-label and image-text data or both. UniTAB (Yang et al., 2022b) employs a transformer based encoder-decoder framework which can jointly output open-ended text and box encouraging alignment between words and boxes. FIBER (Dou et al., 2022a) fuses vision and language encoder backbones through merged co-attention which are then pre-trained on 4M data with two stage pre-training (coarse- and fine-grained). Image-text pairs are used in the coarse-grained pre-training stage which is then followed by a fine-grained pre-training stage with image-text-box annotations. However, these bounding box annotations come with extra overheads. Therefore, in our model, VoLTA, we propose an alternate solution for optimal-transport based local feature-level alignment using global image-caption annotations which performs well not only on coarse-grained tasks (such as VQA and Image Captioning), but also on fine-grained tasks (such as Referring Expression Comprehension and Object Detection). Table B.1 encapsulates an overview of the details of all these aforementioned methods.

C DOWNSTREAM DATASETS

Our downstream tasks can be categorized into three groups: uni-modal, multi-modal coarse-grained, and multi-modal fine-grained.

Uni-modal: For uni-modal tasks, we fine-tune (and validate) our pre-trained model on ImageNet-1k (Deng et al., 2009) for Image Classification, VOC07+12 (Everingham et al., 2010) for image classification and object detection, and COCO (Lin et al., 2014) for image classification, object detection and instance segmentation.

Multi-modal Coarse-grained: Here, we fine-tune (and validate) our pre-trained model on VQAv2 (Antol et al., 2015) for visual question answering, NLVR² (Suhr et al., 2019) for visual reasoning, Flickr30k (Plummer et al., 2015) for image and text retrieval, and COCO (Lin et al., 2014) for image captioning.

Multi-modal Fine-grained: For these tasks, we fine-tune (and validate) our pre-trained model on RefCOCO, RefCOCO+, and RefCOCOg (Kazemzadeh et al., 2014; Yu et al., 2016) for referring expression comprehension, and COCO (Lin et al., 2014) and LVIS Mini (Gupta et al., 2019) for language-conditioned object detection.

It is to be noted that several multi-modal downstream tasks are built based on the COCO dataset where the validation and test splits of these tasks are scattered across the raw COCO splits. Therefore, when pre-training our model, we carefully selected the portion of the COCO dataset which does not overlap with the validation/test splits of these multi-modal downstream tasks.

D IMPLEMENTATION DETAILS & HYPER-PARAMETER VALUES

D.1 DATA AUGMENTATION

We use ResNet50/Swin-T/Swin-B (He et al., 2016; Liu et al., 2021) as image encoder and RoBERTa (Liu et al., 2019) as text encoder. Encoders are followed by a corresponding projector network which is a 3-layer MLP with the configuration [d -2048-2048-1024] where d represents the embedding dimension of the encoder’s output.

Table D.1: **Image and text augmentation details.**

Data Type	View #	Augmentation	Probability
Image	1	RandomResizedCrop	1.0
	1	RandomHorizontalFlip	0.5
	1	ColorJitter	0.8
	1	RandomGrayscale	0.2
	1	GaussianBlur	1.0
	1	Solarization	0.0
	2	RandomResizedCrop	1.0
	2	RandomHorizontalFlip	0.5
	2	ColorJitter	0.8
	2	RandomGrayscale	0.2
Text	1	GaussianBlur	0.1
	1	Solarization	0.2
	1	Synonym Replacement	0.1
	1	Random Insertion	0.1
	1	Random Swap	0.1
	1	Random Deletion	0.1
	2	Synonym Replacement	0.1
	2	Random Insertion	0.2
	2	Random Swap	0.1
	2	Random Deletion	0.2

Image Augmentations: Two sets of random transformations sampled from an augmentation pool are applied on each input image to generate two disparate distorted views. The augmentation policy is composed of RandomResizedCrop, RandomHorizontalFlip, ColorJitter, RandomGrayscale, GaussianBlur, and Solarization augmentations where RandomResizedCrop is applied with a probability of 1.0, whilst the remaining ones are applied randomly with varying probabilities following Zbontar et al. (2021) as outlined in Table D.1.

Text Augmentations: Two sets of random transformations are applied on input text using EDA (Wei & Zou, 2019) including synonym replacement, random insertion, random swap, and random deletion with different probabilities as outlined in Table D.1.

D.2 PRE-TRAINING SETUP

Table D.2 shows the details of hyper-parameters used during training.

Our proposed VLP model, VoLTA comprises a vision encoder and a language encoder with a merged co-attention for cross-modality fusion. While conducting experiments, we have considered two types of vision encoder backbones - ResNet-50 (He et al., 2016) and Swin Transformer (Liu et al., 2021). It is to be noted that for fair comparisons with related works (Dou et al., 2022b;a), the input image resolution for ResNet-50 encoder backbone is kept as 224×224 , whereas for Swin-B, it is 384×384 . The output embedding dimension of the image encoder in both cases is 1024. Similarly, to be consistent with Dou et al. (2022b;a), we have selected RoBERTa as the language encoder with vocabulary size of 50265, tokenizer as 'roberta-base', maximum input text length of 30, and an output embedding dimension of 768 (please refer to Table D.2 for more details).

Vision and language encoders are individually followed by projector heads, each consisting of 3 linear layers each with 2048 output units (except for the last one which has 1024 output units) accompanied with a Batch Normalization layer and ReLU activation (for exact configuration please refer to Table D.2). The final projected output denotes the feature representation of the input (image and/or text) which are used for downstream tasks. In order to learn these representations, the embeddings (i.e., output from respective encoders) are fed to the loss function of VoLTA.

The loss function of VoLTA includes four different loss components, namely, multi-modal Barlow Twins for intra- and inter-modality redundancy reduction, GOT for alignment of local features, MLM and ITM together for encouraging cross-modal attention fusion. For MLM, we randomly mask 15% (MLM probability in Table D.2) of the input tokens and the model is trained to reconstruct the original tokens. For ITM, the model predicts whether a given image-text pair is matched.

For optimization, we follow the same protocol as described in Zbontar et al. (2021) where we use the LARS (You et al., 2017) optimizer to train our model for 20 epochs with a batch size of 256. A base LR of 0.1 is used for the weights and 0.0048 for the biases and batch normalization parameters which are then multiplied by a factor of 2. We employ a learning rate warm-up (linear) upto a period of 2 epochs followed by a cosine decay schedule to reduce the LR by a factor of 1000. A weight decay parameter of 1e-6 is used excluding the biases and batch normalization parameters. We conducted grid search for the GOT loss hyperparameter (w_{GOT}) and we empirically found the best value to be 100.

Pre-training cost: Our Swin-B backbone takes 6 hours per epoch to train on 64 V100 GPUs, with per GPU batch-size 4.

D.3 DOWNSTREAM SETUP

D.3.1 UNI-MODAL DOWNSTREAM TASKS

Linear Evaluation: For ImageNet, the linear classifier has been trained for 100 epochs with batch size of 256, LR of 0.3 and a cosine LR schedule. Cross-entropy loss is minimized with SGDM optimizer (momentum of 0.9) and a weight decay of 1e-6. For both COCO and VOC, the linear classifier has been trained for 100 epochs with AdamW optimizer with batch size of 256, LR of 5e-2 and a weight decay of 1e-6.

Object Detection: For training the detection model, the detectron2 library (Wu et al., 2019) has been used. The backbone networks for Faster R-CNN (Ren et al., 2015) and Mask R-CNN (He et al., 2017) has been initialized using our pre-trained model.

For VOC07+12, we used the `trainval` set comprising of 16K images for training a Faster R-CNN (Ren et al., 2015) C-4 backbone for 24K iterations using a batch size of 16 across 8 GPUs using SyncBatchNorm. The initial learning rate for the model is 0.15 which is reduced by a factor of 10 after 18K and 22K iterations. Linear warmup (Goyal et al., 2017) is used with a slope of 0.333 for 1000 iterations.

For COCO, Mask R-CNN (He et al., 2017) with a C-4 backbone on the COCO 2017 train split is used for training and the results are reported on the val split. A learning rate of 0.03 is used and the other parameters are kept the same as in the $1 \times$ schedule in detectron2 (Wu et al., 2019).

Table D.2: Pre-training hyper-parameter details for VoLTA.

Hyper-parameters	Notation	Value
Model		
Img. proj. layer config.	-	$[d_i - 2048 - 2048 - 1024]$
Img. embed. dim	d_i	1024
Img. reso. (RN-50 & Swin-T)	-	224×224
Img. reso. (Swin-B)	-	384×384
Txt. proj. layer config.	-	$[d_t - 2048 - 2048 - 1024]$
Txt. embed. dim	d_t	768
Tokenizer	-	'roberta-base'
Vocab size	-	50265
MLM prob.	-	0.15
Max. length of text	-	30
# Heads of Xformer	-	12
# Layers of Xformer	-	12
# Fusion block	-	6
Dropout rate	-	0.1
Task names	-	'BTGOT, MLM, ITM'
Training		
Batch size	-	256
Epochs	-	20
Lambda_BT	λ	0.005
WD and GWD loss weight	γ	0.1
GOT loss weight	w_{GOT}	100.0
Optimizer	-	LARS
Base LR for weights	-	0.1
Base LR for biases	-	0.0048
Momentum	-	0.9
LR scheduler	-	Cosine LR decay (with linear warm-up)
Warm-up steps	-	$2 \times \text{Epochs}$
Weight decay	-	1e-6
End LR factor	-	0.001
Cosine LR amplitude factor	-	0.5

D.3.2 COARSE-GRAINED MULTI-MODAL DOWNSTREAM TASKS

Vision-Language Classification (VQAv2 and NLVR²): Vision-Language Classification task encompasses VQAv2 and NLVR² whose hyper-parameter setup has been taken from METER (Dou et al., 2022b) and FIBER (Dou et al., 2022a). Model finetuning is done with peak learning rates of 2e-5 for the backbones, 1e-4 for the cross-modal parameters, and 1e-3 for the head layer for 10 epochs with a batch size of 512. The image resolutions are set to 576 for VQAv2 and 384 for NLVR² and the models are evaluated with the VQA-Scores for VQAv2 and accuracy for NLVR² (Table C.1).

Image-Text Retrieval (IRTR): We follow Dou et al. (2022a) for IR-TR setup for the Flickr30k dataset where the cross-attention layers in the backbones are removed during IR-TR fine-tuning and evaluation. The peak learning rates are set to 2e-5 for the backbones and 1e-4 for the head layer, a batch size of 1024 is considered and each image resolution is set to 576. We evaluate on the Recall@1 metric for both text and image retrieval tasks as outlined in the Table C.1.

Image Captioning: For image captioning, only the image-to-text attentions are kept for the cross-modality attention fusion and the model is converted into a standard seq2seq model (Dou et al., 2022a). We used causal mask in the decoding side and the outputs are predicted auto-regressively (Dou et al., 2022a). Models are trained with the cross-entropy loss for 5 epochs with the peak learning rates of 5e-5 for the backbones, and 2.5e-4 for the rest of the parameters followed by a two-stage finetuning. In the first stage, finetuning with GOLD (Pang & He, 2021) is done for 5 epochs with a peak learning rate of 1e-5 for the backbones, since it is efficient and has been proven to be effective when the model input can correspond to different outputs. Second stage finetuning involves CIDEr optimization where the learning rate is further reduced to 1e-6 and the model is trained for 3 epochs.

Table E.1: **Ablation study on different losses of the training objective of VoLTA for multi-modal coarse-grained downstream tasks.** Each model is pre-trained on 123k train-val samples from COCO2017. For captioning, reported results are for VoLTA-GOLD-B without CIDEr optimization. VoLTA-GOLD-B denotes Swin-B backbone with GOLD (Pang & He, 2021).

VoLTA				VQAv2		NLVR ²		F30k IRTR		Captioning			
\mathcal{L}_{BT}	\mathcal{L}_{GOT}	\mathcal{L}_{MLM}	\mathcal{L}_{ITM}	dev	std	dev	test-P	IR@1	TR@1	B@4	M	C	S
✓	—	—	—	70.3	70.8	68.0	69.7	62.7	75.9	37.3	28.5	124.2	22.1
✓	✓	—	—	71.7	72.5	68.3	68.9	63.1	77.1	37.3	28.9	125.0	22.2
✓	✓	✓	✓	72.8	72.9	69.1	72.9	64.4	78.6	38.4	29.8	126.6	22.4

Table E.2: **Ablation study on different losses of the training objective of VoLTA for referring expression comprehension tasks.** Each model is pre-trained on 123k train-val samples from COCO2017.

VoLTA				RefCOCO			RefCOCO+			RefCOCOg	
\mathcal{L}_{BT}	\mathcal{L}_{GOT}	\mathcal{L}_{MLM}	\mathcal{L}_{ITM}	val	testA	testB	val	testA	testB	val	test
✓	—	—	—	81.0	82.3	76.9	70.3	75.7	60.9	69.2	68.3
✓	✓	—	—	82.9	85.1	78.3	72.1	78.0	64.3	72.1	72.0
✓	✓	✓	✓	83.9	86.3	79.4	73.5	78.8	65.5	73.2	72.9

A batch size of 512 is considered in both these cases and a beam size of 5 is used during inference. Evaluation metrics include BLEU (Papineni et al., 2002), METEOR (Banerjee & Lavie, 2005), CIDEr (Vedantam et al., 2015), and SPICE (Anderson et al., 2016) scores as shown in Table C.1.

D.3.3 FINE-GRAINED MULTI-MODAL DOWNSTREAM TASKS

Referring Expression Comprehension (REC): We follow Dou et al. (2022a) for training and evaluation on 3 different datasets (RefCOCO, RefCOCO+, and RefCOCO) where the models are finetuned with a batch size of 16 for 20 epochs. A warmup of 2000 steps with a peak LR of 1e-5 for both the OD head as well as the rest of the model’s parameters are used. LR drops twice, once at 67% and the other at 89% of the total number of steps. Horizontal flip augmentation has been turned off during REC training because it was observed in Dou et al. (2022a) that horizontal flip adversely affected the performance, particularly on the RefCOCO dataset. Accuracy is used as the evaluation metric in this case (Table C.1).

Object Detection: We follow the training and evaluation setup of Dou et al. (2022a) for text-conditioned (multi-modal) object detection. For both COCO and LVIS datasets, model has been finetuned for 24 epochs with batch size of 32, a LR of 1e-5, and two learning rate drops, once at 67% and the other at 89% of the total number of steps. AP scores are used in this case for model evaluation (Table C.1).

E ABLATION

We have conducted ablation studies, particularly, on pre-training objectives, GOT loss weight and the dimension of projectors which are summarized below:

E.1 ABLATION ON PRE-TRAINING OBJECTIVE

We analyze the effectiveness of different pre-training objectives through an ablation on coarse- and fine-grained downstream tasks (Tables E.1 and E.2). Adding GOT loss on top of multi-modal BT boosts downstream performance. This result suggests that the fine-grained cross-modal alignment between image and text features learned through GOT during pre-training helps region-level downstream tasks. Next, we add MLM and ITM loss which helps the model to learn cross-modal information via attention fusion. This final addition substantially improved our model’s overall performance on coarse and fine-grained tasks.

Table E.3: **Ablation study on the value of w_{GOT} , the weight of GOT loss in $\mathcal{L}_{\text{total}}$ in the objective of VoLTA for multi-label image classification on VOC07 and COCO.** We report classification mAP on VOC07, and per-class (PC) and overall (O) F1 scores on COCO. Each model is pre-trained on 123k train-val samples from COCO2017.

w_{GOT}	VOC07	COCO
	MLP	MLP (PC/O)
50	93.4	74.1/76.0
100	94.0	74.5/76.4
200	93.2	73.1/75.5
500	93.1	72.8/75.3

Table E.4: **Ablation study on the dimension of local and global projector networks of VoLTA for multi-label image classification on VOC07 and COCO.** We report classification mAP on VOC07, and per-class (PC) and overall (O) F1 scores on COCO. Each model is pre-trained on 123k train-val samples from COCO2017.

Projector Config.	VOC07	COCO
	MLP	MLP (PC/O)
8192-8192-128	91.3	71.3/73.0
8192-8192-256	91.9	72.2/73.3
2048-2048-512	93.4	73.9/76.1
2048-2048-1024	94.0	74.5/76.4

E.2 ABLATION ON GOT LOSS WEIGHT

In our loss formulation, we introduce a GOT loss weight w_{GOT} which regulates the alignment of local features through GOT loss. By conducting a grid-search on uni-modal downstream classification tasks, we assessed the impact of w_{GOT} as shown in the Table E.3 and experimentally found its best value to be 100 in our case. It is to be noted that a very high value of w_{GOT} considerably degrades the performance on downstream tasks.

E.3 ABLATION ON PROJECTOR DIMENSION

The design of projector head plays a pivotal role in the downstream performance of the model (Garrido et al., 2022). To investigate the impact of hidden and feature (projector output) dimensions, we have tested 4 different configurations on uni-modal downstream classification tasks. It can be noticed from Table E.4 that an increase in the number of parameters in the projector head does not necessarily lead to an increase in performance. For example, a projector configuration of 8192-8192-256 has roughly 8 times more parameters than 2048-2048-1024, although, the latter performs better in downstream tasks (Table E.4), indicating that the output (feature) dimension of projector plays a crucial role in final performance of the model.

F RESULTS ON COARSE-GRAINED VISION LANGUAGE TASKS: COMPARISON WITH METHODS USING MORE PRE-TRAINING DATA

Table F.1 presents a comparison of VoLTA on multimodal coarse-grained tasks with state-of-the-art methods pre-trained using magnitude more data. On VQA, VoLTA beat ViLBERT, UNITER-B, and ViLT-B, each pre-trained on 3 – 4M datasets. Note that VoLTA is trained only on COCO, whereas the other methods use a combination of COCO, VG, CC, and SBU datasets. Such strong performance proves the generalizability of VoLTA. On captioning, VoLTA beats Unified VLP, OSCAR, UFO-B, ViTCAP, and XGPT. However, for IRTR and NLVR, VoLTA can not yield better performance over these baselines. We assume that the large domain difference between pre-training and downstream datasets is the reason behind the limited performance.

G QUALITATIVE RESULTS

Visual Question Answering and Visual Reasoning: Visual question answering (VQA) is a widely recognized multi-modal task which infers an answer in response to a text-based question about an im-

Table F.1: **Multi-modal coarse-grained downstreams: visual question answering, visual reasoning, retrieval and captioning.** Methods pre-training with significantly larger dataset are colored gray. For captioning, 4 metrics are reported - B@4: BLEU@4, M: METEOR, C: CIDEr, S: SPICE. Best comparable results are in **bold**. VoLTA-B denotes Swin-B backbone.

Method	#Pre-train Images	VQAv2		NLVR ²		F30k IRTR		Method	#Pre-train Images	COCO Captioning									
		dev	std	dev	test-P	IR@1	TR@1			B@4	M	C	S						
<i>Models pre-trained on COCO (123k) and/or VG (108k)</i>																			
SCAN	108k	—	—	—	—	48.6	67.4	VL-T5	180k	34.5	28.7	116.5	21.9						
SCG	108k	—	—	—	—	49.3	71.8	VL-BART	180k	35.1	28.7	116.6	21.5						
PFAN	108k	—	—	—	—	50.4	70.0	Unified VLP	3M	36.5	28.4	117.7	21.3						
MaxEnt	123k	54.1	54.8	—	—	—	—	OSCAR	4M	36.5	30.3	123.7	23.1						
VisualBERT	123k	70.8	71.0	67.4	67.0	—	—	UFO-B	4M	36.0	28.9	122.8	22.2						
LXMERT	231k	72.4	72.5	74.9	74.5	—	—	ViTCAP	4M	36.3	29.3	125.2	22.6						
<i>Models pre-trained on COCO, VG, SBU (1M) and/or CC (3M)</i>																			
ViLBERT	3M	70.5	70.9	—	—	58.2	—	ViLBERT	3.1M	37.2	28.6	120.1	21.8						
UNITER-B	4M	72.7	72.9	77.2	77.9	72.5	85.9	FIBER-B	4M	39.1	30.4	128.4	23.1						
VILLA-B	4M	73.6	73.7	78.4	79.3	74.7	86.6	FIBER-GOLD-B	4M	40.3	30.7	133.6	23.6						
UNIMO-B	4M	73.8	74.0	—	—	—	—	VoLTA-GOLD-B	123k	38.4	29.8	126.6	22.4						
ViLT-B	4M	71.3	-	75.7	76.1	64.4	83.5	<i>Models fine-tuned with CIDEr optimization</i>											
ALBEF-B	4M	74.5	74.7	80.2	80.5	82.8	94.3	ViTCAP	4M	41.2	30.1	138.1	24.1						
VLMo-B	4M	76.6	76.9	82.8	83.3	79.3	92.3	ViNL-B	4M	40.9	30.9	140.4	25.1						
METER-Swin-B	4M	76.4	76.4	82.2	83.5	79.0	92.4	FIBER-B	4M	42.8	31.0	142.8	24.3						
FIBER-B	4M	78.6	78.4	84.6	85.5	81.4	92.9	FIBER-GOLD-B	4M	43.4	31.3	144.4	24.6						
VoLTA-B	123k	72.8	72.9	69.1	72.9	64.4	78.6	VoLTA-GOLD-B	123k	39.8	30.5	137.5	23.6						

age. In Figure G.1 we demonstrated several example image-question pairs along with corresponding answers predicted by VoLTA on VQAv2 validation set. The primary aim of the visual reasoning task is to ascertain the veracity of a natural language statement against an associated image pair. Figure G.2 displays examples of responses (True/False) predicted by VoLTA on NLVR² validation set.

Language-conditioned Object Detection: Object detection forms an indispensable constituent of several multi-modal understanding systems. However, conventional object detection pipeline, being employed as a black-box tool, predicts all possible objects in the image. On the other hand, for better apprehension of combinations of these objects in free-form texts, language-conditioned object detection task is considered (Kamath et al., 2021; Dou et al., 2022a). We use pre-trained VoLTA for fine-tuning and evaluation on COCO and LVIS datasets for text-conditioned object detection task. As illustrated in the Figure G.3, VoLTA predicts bounding boxes relevant to the text prompts (captions) and labels them with the corresponding spans from the text. For example, the top-middle image has 4 objects, however our model predicts boxes only for *person* and *cup* based on the text prompt.

Referring Expression Comprehension (REC): The objective of REC is to align the entire referring expression (text) with the corresponding box by disambiguating among the several occurrences of an object belonging to the same category and therefore, one box per expression is to be predicted. For example, bottom-left image in Figure G.4 depicts VoLTA’s box prediction for the corresponding referring expression: *the slice of cake on the left*.

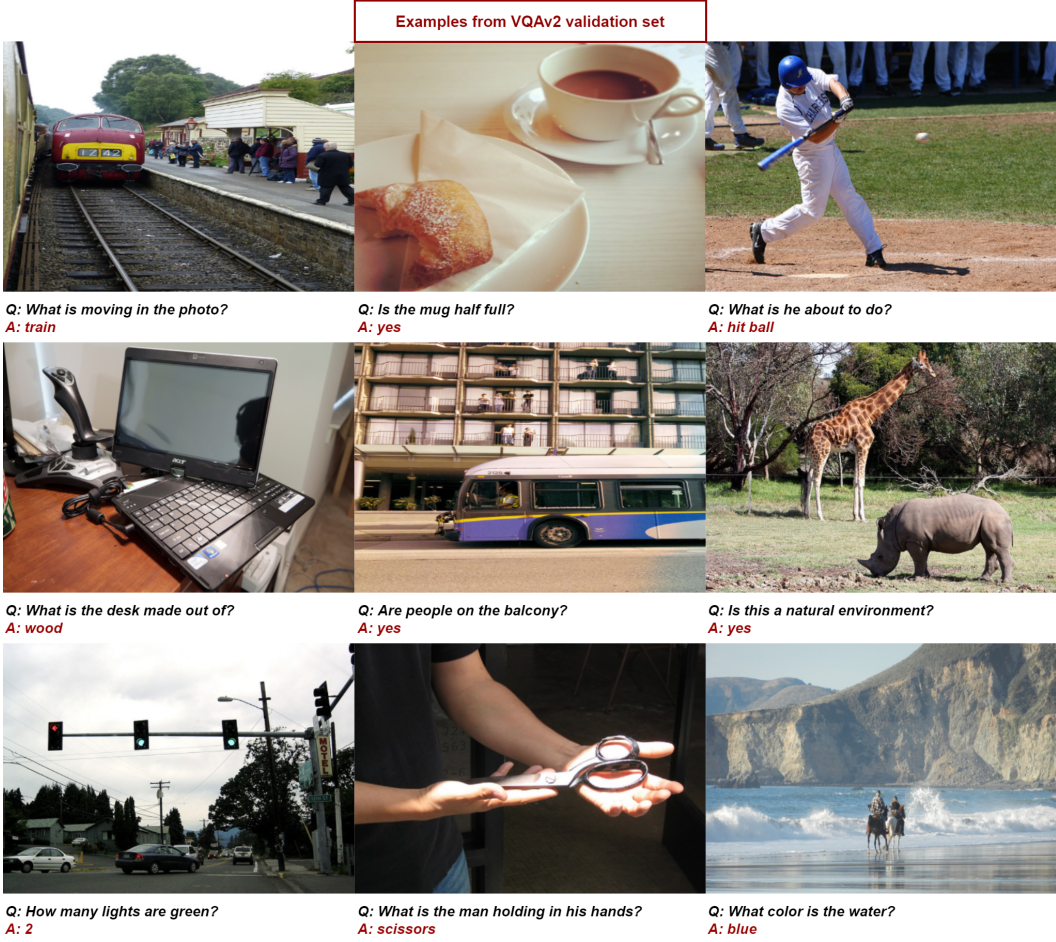


Figure G.1: **Examples on Visual Question Answering from VQAv2 validation dataset.** We display a variety of examples (e.g., number of items, color of objects, type of objects, events and actions) with respective answers predicted by VoLTA.



Figure G.2: **Examples on Visual Reasoning from NLVR² validation dataset.** For each statement (text prompt), 2 images are shown alongside each other and VoLTA predicts whether the given statement is True (green box) or False (red box).



Figure G.3: **Examples of Object Detection from COCO validation dataset with various text prompts.** Our model predicts boxes relevant to the text (caption) and labels them with the corresponding spans.



Figure G.4: **Examples of Referring Expression Comprehension from RefCOCO (top), RefCOCO+ (middle) and RefCOCOg (bottom) validation datasets.** The expressions in RefCOCOg typically have florid and longer constructions as compared to RefCOCO and RefCOCO+. The model has access to the entire text and uses it to disambiguate amongst different objects in the image.

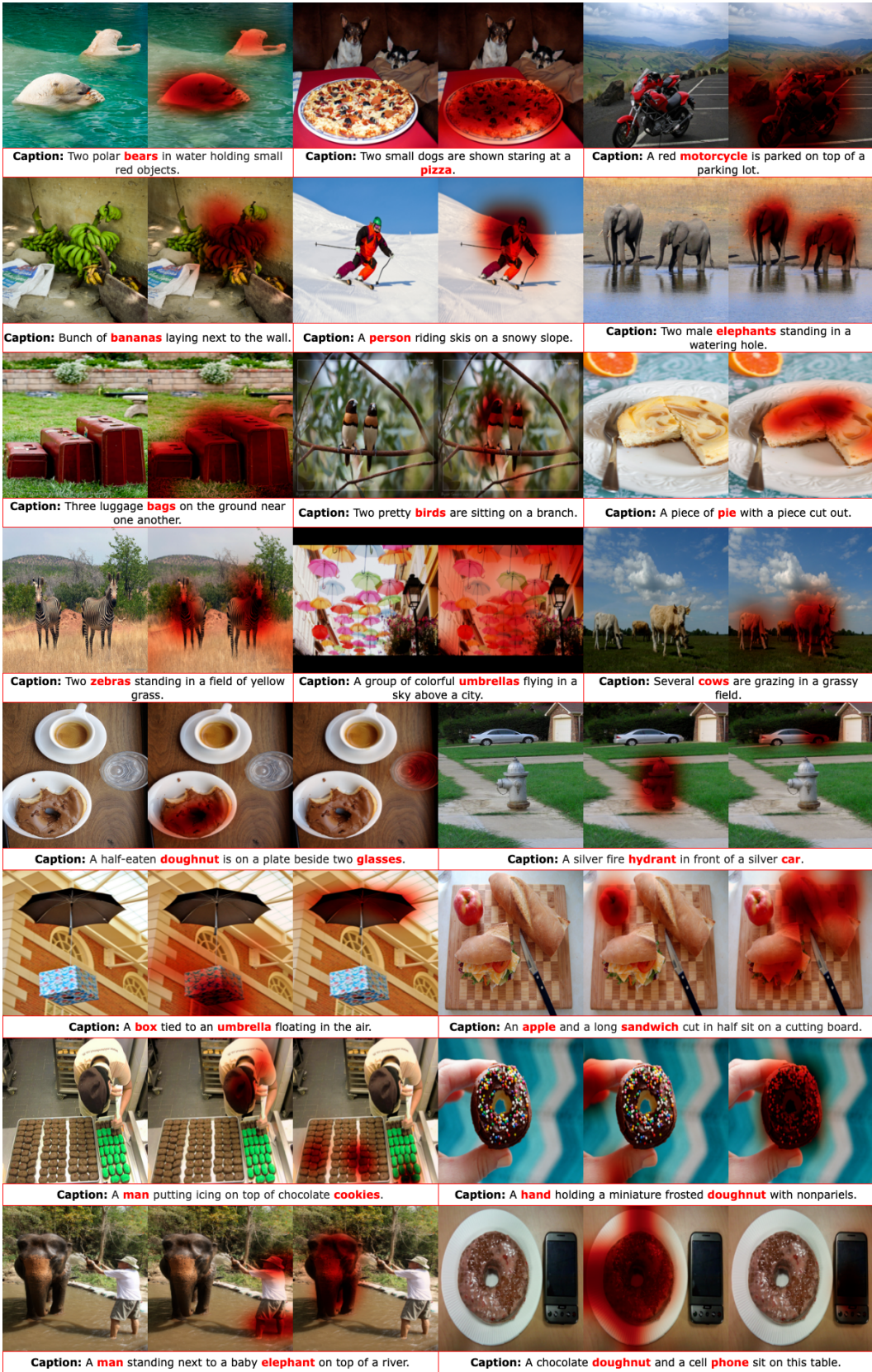


Figure G.5: This figure shows how different words in captions attend relevant image regions, produced by the GOT module of VolTA pre-trained on COCO. Extension of Figure 1. All image-caption pairs are taken from the COCO2017 train split.